International Journal of Solids and Structures 41 (2004) 5565–5594

INTERNATIONAL JOURNAL OF SOLIDS and STRUCTURES

www.elsevier.com/locate/ijsolstr

# Nonlinear normal modes of structural systems via asymptotic approach

Walter Lacarbonara [a,*], Rodolfo Camillacci [b]

[a] *Dipartimento di Ingegneria Strutturale e Geotecnica, Università di Roma La Sapienza, via Eudossiana 18, Rome 00184, Italy*
[b] *Dipartimento di Scienze dell'Ingegneria Civile, Università di Roma Tre, via Vito Volterra 62, Rome 00146, Italy*

Received 12 January 2004; received in revised form 9 April 2004
Available online 1 June 2004

**Abstract**

An asymptotic approach, based on the method of multiple scales, is employed to construct the nonlinear normal modes (NNM's) of self-adjoint structural systems with arbitrary linear inertia and elastic stiffness operators, general cubic inertia and geometric nonlinearities. The methodology employed for constructing the approximate invariant manifolds of individual NNM's—away from internal resonances—and of the resonant modes—near three-to-one internal resonances—attempts to generalize previous studies based on asymptotic techniques. The theory is applied to a hinged–hinged uniform elastic beam carrying a lumped mass and undergoing axis stretching. Depending on the lumped mass relative to the beam mass and on its position along the span, different classes of nonlinear normal modes and their stability are investigated.


*Keywords:* Nonlinear normal modes; Model reduction; Structural dynamics; Asymptotics; Nonlinear beam; Method of multiple scales

## 1. Introduction

The theory of normal modes of vibration is well established for linear oscillatory systems. The linear normal modes, defined as eigenvectors (eigenfunctions) of the governing linear differential (partial-differential) problem, remarkably lead to the expansion theorem allowing to express an arbitrary response as a superposition of modal contributions. Another distinguished modal property, the invariance, often allows for the reduction of the modeled modes.

The idea of extending the concept of normal modes to nonlinear systems was first proposed by Rosenberg (1962, 1966) for finite-degree-of-freedom systems. Rand (1974), Rand et al. (1992), Vakakis and Rand (1992), and Vakakis et al. (1996) have made important contributions to the problem of defining theoretically and constructing analytically the nonlinear normal modes.

* Corresponding author. Tel.: +39-6-44585293; fax: +39-6-4884852.
*E-mail address:* walter.lacarbonara@uniromal.it (W. Lacarbonara).

0020-7683/$ - see front matter 
doi:10.1016/j.ijsolstr.2004.04.029

Shaw and Pierre (1991, 1993) introduced the concept of nonlinear normal modes as low-dimensional (typically, two-dimensional) invariant-manifolds tangent to the hyperplane spanned by the linear modes in the phase space. They used a real-valued invariant-manifold approach to construct the nonlinear normal modes of conservative as well as nonconservative vibratory finite-degree-of-freedom systems away from internal resonances. The nonlinear mode shapes were determined in a manner similar to center manifold reduction borrowed from bifurcation theory. Pesheck et al. (2001) extended the invariant-manifold method also to the case of internal resonances.

Nayfeh and Nayfeh (1994, 1995) used a complex-valued invariant-manifold approach to construct the nonlinear normal modes of multi-degree-of-freedom systems with quadratic and cubic nonlinearities. Nayfeh et al. (1996) extended this approach to the cases of one-to-one and three-to-one internal resonances. A comparison of different approximate methods for constructing the nonlinear normal modes of discrete systems can be found in Camillacci (2003).

Several methods have also been proposed for weakly nonlinear distributed-parameter systems; they include the energy method of King and Vakakis (1993, 1996), the method of harmonic balance, treatments of a discretized version, and direct methods.

With the discretization approach one assumes the solution as an expansion in terms of basis functions from a complete set and then uses one of the variants of the method of weighted residuals to obtain an infinite set of ordinary-differential equations. The infinite set of equations is truncated to practically compute the nonlinear normal modes. Then, the discretized equations are treated with the real-valued or complex-valued form of the invariant-manifold approach, the energy approach, or an asymptotic method. King and Vakakis (1996) used the energy approach to compute the nonlinear normal modes of a hinged–clamped beam in the case of a three-to-one internal resonance between the lowest two modes. They performed a convergence study for various modal truncations and obtained sufficiently accurate solutions by considering the lowest nine modes. They found either one or three nonlinear modes; using Floquet theory it was predicted that, at a given detuning, one mode is unstable and the other two modes are stable.

On the other hand, direct analytical techniques, such as the method of harmonic balance or the method of multiple scales, have also been used to construct the nonlinear normal modes of continuous systems. These techniques do not require an a priori assumption of the form of the solution. Pak et al. (1992), King and Vakakis (1993), Shaw and Pierre (1994), Nayfeh (1995), Nayfeh et al. (1999), Lacarbonara et al. (2003), and Lacarbonara and Rega (2003) used this approach to determine the nonlinear modes of several one-dimensional spatially continuous systems.

In this paper, an asymptotic approach, based on the method of multiple scales, is employed to construct the individual as well as the resonant nonlinear normal modes of self-adjoint structures with general symmetric nonlinearities of the geometric and inertia type. Asymmetric nonlinearities—such as quadratic nonlinearities—have not been here considered because the reference mechanical systems (e.g., shear-type building structures) belong to the class of structural systems where the symmetric restoring forces are dominant. With symmetric and asymmetric nonlinearities, the methodology could be conveniently modified as done in the general context of distributed-parameter systems discussed in Lacarbonara et al. (2003) and Lacarbonara and Rega (2003).

In the present work, the achieved outcomes are the invariant physical manifolds associated with the modes, the mode shapes (nonlinear eigenvectors) and the nonlinear frequency dependence on the vibration amplitude. With respect to previous studies based on the method of multiple scales (Nayfeh, 1995; Nayfeh et al., 1999; Lacarbonara et al., 2003; Lacarbonara and Rega, 2003), here the methodology is developed and discussed in a systematic format including the fundamental steps leading to the nonlinear mode shapes. These are obtained as an extension of the linear eigenvectors and, more importantly, the extent of the nonlinear corrections is discussed and interpreted mechanically resorting to the concept of virtual work.

Further, the generated results are system-independent and as such they can be suitably exploited for nonlinear modal-type analyses of general nonlinear structural systems. In fact, as the normal modes of linear systems are conveniently used in modal analyses, the concept of nonlinear normal modes of vibration suggests the definition of a nonlinear modal analysis (Pesheck et al., 2001) whereby an arbitrary nonlinear vibratory response of a structural system is obtained in terms of nonlinear modal coordinates. As model reduction is performed for linear systems, model reduction is also expected to be possibly achieved using the nonlinear normal coordinates with the goal of employing the least number of nonlinear modes relative to the number of linear modes needed to achieve a comparable accuracy in modal-type analyses of nonlinear systems.

The case of a hinged–hinged uniform elastic beam carrying a lumped mass is discussed as an illustrative example. The closed-form nonlinear modes are either individual, away from internal resonances, or resonant, in the vicinity of three-to-one internal resonances. The differences between the linear normal modes and their nonlinear companions are discussed. In the case of resonant nonlinear normal modes, the bifurcation behavior is studied varying the internal detuning parameter.

The paper is organized as follows. In Sections 2–4, the asymptotic approach for generating the nonlinear normal modes of general structures is presented. Section 5 shows the main results relating to the illustrative problem; finally, the summary and concluding remarks are presented in Section 6.

## 2. General self-adjoint structural systems: computational approach

In this section, the asymptotic method of multiple scales is employed to construct the nonlinear normal modes of multi-degree-of-freedom self-adjoint structures described by the following nondimensional vector-valued equation of motion:

$$\mathbf{M}\ddot{\mathbf{x}} + \mathbf{K}\mathbf{x} + \mathbf{K}_3(\mathbf{x},\mathbf{x},\mathbf{x}) + \mathbf{M}_3(\mathbf{x},\dot{\mathbf{x}},\dot{\mathbf{x}}) + \mathbf{M}_3^*(\mathbf{x},\mathbf{x},\ddot{\mathbf{x}}) = \mathbf{0} \tag{1}$$

where $\mathbf{M}$ and $\mathbf{K}$ are $N \times N$ symmetric and positive-definite matrices representing the linear mass and stiffness operators, respectively; $\mathbf{x}$ is the $N \times 1$ vector of the nondimensional generalized coordinates; $\mathbf{K}_3$, $\mathbf{M}_3$ and $\mathbf{M}_3^*$ are $N \times 1$ noncommutative and multilinear operators which represent the nonlinear cubic stiffness ($\mathbf{K}_3$) and nonlinear inertia ($\mathbf{M}_3, \mathbf{M}_3^*$), respectively; and the dot denotes differentiation with respect to the nondimensional time $t$. While the geometric nonlinearities arise from the nonlinear strain–displacement relations, the inertia nonlinearities of the assumed form are typical of inextensible systems. The dynamic structural model represented by Eq. (1) is supposed to be accurate, kinematically and constitutively, so as to be capable of capturing the physical structural behaviors under investigation also for high frequencies.

Let $\mathbf{B}_0$ represent the linear modal tensor such that, introducing the transformation $\mathbf{x} = \mathbf{B}_0\mathbf{q}$, the set of equations (1) can be rewritten in the modal coordinates $q_j$ as

$$\ddot{\mathbf{q}} + \mathbf{\Lambda}\mathbf{q} = \mathbf{G}_3(\mathbf{q},\mathbf{q},\mathbf{q}) + \mathbf{I}_3(\mathbf{q},\dot{\mathbf{q}},\dot{\mathbf{q}}) + \mathbf{I}_3^*(\mathbf{q},\mathbf{q},\ddot{\mathbf{q}}) \tag{2}$$

where

$$\mathbf{\Lambda} = \mathbf{B}_0^{\mathrm{T}}\mathbf{K}\mathbf{B}_0 = \begin{bmatrix} \omega_{01}^2 & \cdots & 0 \\ \vdots & \ddots & \vdots \\ 0 & \cdots & \omega_{0n}^2 \end{bmatrix} \tag{3}$$

and $\mathbf{B}_0$ has been normalized such that $\mathbf{B}_0^{\mathrm{T}}\mathbf{M}\mathbf{B}_0 = \mathbf{I}$, with $\mathbf{I}$ being the identity tensor and T indicating the transpose. The assumption that the frequencies are distinct has been made; moreover, $\mathbf{G}_3(\mathbf{q},\mathbf{q},\mathbf{q}) = -\mathbf{B}_0^{\mathrm{T}}\mathbf{K}_3(\mathbf{B}_0\mathbf{q},\mathbf{B}_0\mathbf{q},\mathbf{B}_0\mathbf{q})$; $\mathbf{I}_3(\mathbf{q},\dot{\mathbf{q}},\dot{\mathbf{q}}) = -\mathbf{B}_0^{\mathrm{T}}\mathbf{M}_3(\mathbf{B}_0\mathbf{q},\mathbf{B}_0\dot{\mathbf{q}},\mathbf{B}_0\dot{\mathbf{q}})$; $\mathbf{I}_3^*(\mathbf{q},\mathbf{q},\ddot{\mathbf{q}}) = -\mathbf{B}_0^{\mathrm{T}}\mathbf{K}_3(\mathbf{B}_0\mathbf{q},\mathbf{B}_0\mathbf{q},\mathbf{B}_0\ddot{\mathbf{q}})$.

The second-order (in time) set of equations (2) can be conveniently reduced to a first-order system as follows:

$$\begin{aligned} \dot{\mathbf{q}} &= \mathbf{p} \\ \dot{\mathbf{p}} + \mathbf{\Lambda}\mathbf{q} &= \mathbf{G}_3(\mathbf{q},\mathbf{q},\mathbf{q}) + \mathbf{I}_3(\mathbf{q},\mathbf{p},\mathbf{p}) + \mathbf{I}_3^*(\mathbf{q},\mathbf{q},\dot{\mathbf{p}}) \end{aligned} \tag{4}$$

Introducing a small dimensionless number $\epsilon$ as an ordering device, a third-order expansion of the solutions of (4) is sought in the form

$$\begin{aligned} \mathbf{q} &= \epsilon\mathbf{q}_1(T_0,T_1,T_2) + \epsilon^2\mathbf{q}_2(T_0,T_1,T_2) + \epsilon^3\mathbf{q}_3(T_0,T_1,T_2) + \cdots \\ \mathbf{p} &= \epsilon\mathbf{p}_1(T_0,T_1,T_2) + \epsilon^2\mathbf{p}_2(T_0,T_1,T_2) + \epsilon^3\mathbf{p}_3(T_0,T_1,T_2) + \cdots \end{aligned} \tag{5}$$

where $T_0 = t$ is a fast scale characterizing motions occurring at one of the system natural frequencies $\omega_{0k}$ and $T_j = \epsilon^j t$, $j = 1, 2$, are the slow scales. In terms of $T_j$, the time derivative becomes

$$\frac{\mathrm{d}}{\mathrm{d}t} = D_0 + \epsilon D_1 + \epsilon^2 D_2 + \cdots \tag{6}$$

where $D_j = \partial/\partial T_j$.

Substituting (5) and (6) into (4) and equating the coefficients of like powers of $\epsilon$ yields the following hierarchy of linear problems:

Order $\epsilon$:

$$\begin{aligned} D_0\mathbf{q}_1 - \mathbf{p}_1 &= 0 \\ D_0\mathbf{p}_1 + \mathbf{\Lambda}\mathbf{q}_1 &= 0 \end{aligned} \tag{7}$$

Order $\epsilon^2$:

$$\begin{aligned} D_0\mathbf{q}_2 - \mathbf{p}_2 &= -D_1\mathbf{q}_1 \\ D_0\mathbf{p}_2 + \mathbf{\Lambda}\mathbf{q}_2 &= -D_1\mathbf{p}_1 \end{aligned} \tag{8}$$

Order $\epsilon^3$:

$$\begin{aligned} D_0\mathbf{q}_3 - \mathbf{p}_3 &= -D_1\mathbf{q}_2 - D_2\mathbf{q}_1 \\ D_0\mathbf{p}_3 + \mathbf{\Lambda}\mathbf{q}_3 &= -D_1\mathbf{p}_2 - D_2\mathbf{p}_1 + \mathbf{G}_3(\mathbf{q}_1,\mathbf{q}_1,\mathbf{q}_1) + \mathbf{I}_3(\mathbf{q}_1,\mathbf{p}_1,\mathbf{p}_1) + \mathbf{I}_3^*(\mathbf{q}_1,\mathbf{q}_1,D_0\mathbf{p}_1) \end{aligned} \tag{9}$$

In the next section, the individual nonlinear normal modes are obtained when the structure is away from internal resonances and the resulting invariant manifolds are two-dimensional.

## 3. Individual nonlinear normal modes

Because we are interested in seeking approximations of the $k$th nonlinear normal mode when this mode is away from internal resonances with other modes, the general solution of (7) can be expressed as

$$\begin{aligned} \mathbf{q}_1 &= A_k(T_1,T_2)\mathrm{e}^{\mathrm{i}\omega_{0k}T_0}\mathbf{u}_k + cc \\ \mathbf{p}_1 &= \mathrm{i}\omega_{0k}A_k(T_1,T_2)\mathrm{e}^{\mathrm{i}\omega_{0k}T_0}\mathbf{u}_k + cc \end{aligned} \tag{10}$$

where $\mathbf{u}_k$ is the $k$th eigenvector in the linear modal space (i.e., $u_{kj} = \delta_{kj}$ with $\delta_{kj}$ denoting the Kronecker delta), $\omega_{0k}$ is the $k$th linear frequency, i is the imaginary unit, and $cc$ stands for the complex and conjugate of the preceding terms.

Then, substituting (10) into (8) yields

$$\begin{aligned} D_0\mathbf{q}_2 - \mathbf{p}_2 &= -(D_1A_k)\mathrm{e}^{\mathrm{i}\omega_{0k}T_0}\mathbf{u}_k + cc \\ D_0\mathbf{p}_2 + \mathbf{\Lambda}\mathbf{q}_2 &= -\mathrm{i}\omega_{0k}(D_1A_k)\mathrm{e}^{\mathrm{i}\omega_{0k}T_0}\mathbf{u}_k + cc \end{aligned} \tag{11}$$

Since the homogeneous problem obtained from (11) admits nontrivial solutions, the solvability of (11) is enforced requiring the orthogonality between the solution of the following adjoint homogeneous problem

$$\begin{aligned} D_0\mathbf{q}^* - \mathbf{\Lambda}\mathbf{p}^* &= \mathbf{0} \\ D_0\mathbf{p}^* + \mathbf{q}^* &= \mathbf{0} \end{aligned} \tag{12}$$

and the inhomogeneous term of (11), $\mathbf{g}_1 = -[1, \mathrm{i}\omega_{0k}]^{\mathrm{T}}(D_1A_k)\mathrm{e}^{\mathrm{i}\omega_{0k}T_0}\mathbf{u}_k + cc$.

Because the solution of the adjoint homogeneous problem (12) is

$$\begin{bmatrix} \mathbf{q}^* \\ \mathbf{p}^* \end{bmatrix} = \sum_{j=1}^{N} A_j^* \begin{bmatrix} \mathrm{i}\omega_{0j} \\ 1 \end{bmatrix} \mathrm{e}^{-\mathrm{i}\omega_{0j}T_0}\mathbf{u}_j + cc \tag{13}$$

the orthogonality condition is

$$\int_0^{\tau_k} \mathbf{g}_1^{\mathrm{T}} \begin{bmatrix} \mathbf{q}^* \\ \mathbf{p}^* \end{bmatrix} \mathrm{d}T_0 = 0 \tag{14}$$

where $\tau_k$ is the $k$th period of oscillation. Equation (14) yields $D_1A_k = 0$. This implies that $A_k$ does not depend on the time scale $T_1$; consequently, $A_k = A_k(T_2)$.

Substituting (10) into (9), and accounting for $D_1A_k = 0$, yields

$$\begin{aligned} D_0\mathbf{q}_3 - \mathbf{p}_3 &= -(D_2A_k)\mathrm{e}^{\mathrm{i}\omega_{0k}T_0}\mathbf{u}_k + cc \\ D_0\mathbf{p}_3 + \mathbf{\Lambda}\mathbf{q}_3 &= -\mathrm{i}\omega_{0k}(D_2A_k)\mathrm{e}^{\mathrm{i}\omega_{0k}T_0}\mathbf{u}_k + \left[3\mathbf{G}_3(\mathbf{u}_k,\mathbf{u}_k,\mathbf{u}_k) + \omega_{0k}^2\mathbf{I}_3(\mathbf{u}_k,\mathbf{u}_k,\mathbf{u}_k) - 3\omega_{0k}^2\mathbf{I}_3^*(\mathbf{u}_k,\mathbf{u}_k,\mathbf{u}_k)\right]A_k^2\overline{A}_k\mathrm{e}^{\mathrm{i}\omega_{0k}T_0} \\ &\quad + \left[\mathbf{G}_3(\mathbf{u}_k,\mathbf{u}_k,\mathbf{u}_k) - \omega_{0k}^2\mathbf{I}_3(\mathbf{u}_k,\mathbf{u}_k,\mathbf{u}_k) - \omega_{0k}^2\mathbf{I}_3^*(\mathbf{u}_k,\mathbf{u}_k,\mathbf{u}_k)\right]A_k^3\mathrm{e}^{3\mathrm{i}\omega_{0k}T_0} + cc \end{aligned} \tag{15}$$

where $\overline{A}_k$ stands for the complex and conjugate of $A_k$.

Imposing again the orthogonality between the solution of the adjoint homogeneous problem and the inhomogeneous term of (15), the following modulation equation is obtained:

$$D_2A_k = \frac{\Gamma_{kkk}}{2\mathrm{i}\omega_{0k}}A_k^2\overline{A}_k \tag{16}$$

where

$$\Gamma_{kkk} = 3\mathbf{u}_k^{\mathrm{T}}\mathbf{G}_3(\mathbf{u}_k,\mathbf{u}_k,\mathbf{u}_k) + \omega_{0k}^2\mathbf{u}_k^{\mathrm{T}}\mathbf{I}_3(\mathbf{u}_k,\mathbf{u}_k,\mathbf{u}_k) - 3\omega_{0k}^2\mathbf{u}_k^{\mathrm{T}}\mathbf{I}_3^*(\mathbf{u}_k,\mathbf{u}_k,\mathbf{u}_k) \tag{17}$$

Substituting (16) into (15), the solution of the resulting equation can be expressed as

$$\mathbf{q}_3 = \mathbf{z}_1\mathrm{e}^{\mathrm{i}\omega_{0k}T_0}A_k^2\overline{A}_k + \mathbf{z}_2\mathrm{e}^{3\mathrm{i}\omega_{0k}T_0}A_k^3 + cc \tag{18}$$

$$\mathbf{p}_3 = \mathbf{w}_1\mathrm{e}^{\mathrm{i}\omega_{0k}T_0}A_k^2\overline{A}_k + \mathbf{w}_2\mathrm{e}^{3\mathrm{i}\omega_{0k}T_0}A_k^3 + cc \tag{19}$$

Thereafter, substituting (18) and (19) into (15), and equating the coefficients of $\exp(\mathrm{i}\omega_{0k}T_0)$ and $\exp(3\mathrm{i}\omega_{0k}T_0)$ separately to 0, yields

$$\mathrm{i}\omega_{0k}\mathbf{z}_1 - \mathbf{w}_1 = -\frac{\Gamma_{kkk}}{2\mathrm{i}\omega_{0k}}\mathbf{u}_k \tag{20}$$

$$3\mathrm{i}\omega_{0k}\mathbf{z}_2 - \mathbf{w}_2 = \mathbf{0} \tag{21}$$

$$\mathrm{i}\omega_{0k}\mathbf{w}_1 + \mathbf{\Lambda}\mathbf{z}_1 = -\frac{\Gamma_{kkk}}{2}\mathbf{u}_k + 3\mathbf{G}_3(\mathbf{u}_k,\mathbf{u}_k,\mathbf{u}_k) + \omega_{0k}^2\mathbf{I}_3(\mathbf{u}_k,\mathbf{u}_k,\mathbf{u}_k) - 3\omega_{0k}^2\mathbf{I}_3^*(\mathbf{u}_k,\mathbf{u}_k,\mathbf{u}_k) \tag{22}$$

$$3\mathrm{i}\omega_{0k}\mathbf{w}_2 + \mathbf{\Lambda}\mathbf{z}_2 = \mathbf{G}_3(\mathbf{u}_k,\mathbf{u}_k,\mathbf{u}_k) - \omega_{0k}^2\mathbf{I}_3(\mathbf{u}_k,\mathbf{u}_k,\mathbf{u}_k) - \omega_{0k}^2\mathbf{I}_3^*(\mathbf{u}_k,\mathbf{u}_k,\mathbf{u}_k) \tag{23}$$

Next, the orthogonality is imposed between the solution of the adjoint homogeneous problem and the component of the third-order solution (18) and (19) which is proportional to $\exp(\mathrm{i}\omega_{0k}T_0)$. More concisely, this solvability condition can be written as

$$\begin{bmatrix} \mathrm{i}\omega_{0k}\mathbf{u}_k^{\mathrm{T}} & \mathbf{u}_k^{\mathrm{T}} \end{bmatrix} \begin{bmatrix} \mathbf{z}_1 \\ \mathbf{w}_1 \end{bmatrix} = 0 \tag{24}$$

Substituting Eq. (20) into (24) gives $\mathbf{u}_k^{\mathrm{T}}\mathbf{z}_1 = \Gamma_{kkk}/(4\omega_{0k}^2)$. Consequently, using Eq. (22) gives

$$\mathbf{z}_1 = \frac{\Gamma_{kkk}}{4\omega_{0k}^2}\mathbf{u}_k + \sum_{j=1,j\neq k}^{N}\mathscr{C}_{jk}\mathbf{u}_j, \qquad \mathbf{w}_1 = \mathrm{i}\omega_{0k}\left(-\frac{\Gamma_{kkk}}{4\omega_{0k}^2}\mathbf{u}_k + \sum_{j=1,j\neq k}^{N}\mathscr{C}_{jk}\mathbf{u}_j\right) \tag{25}$$

where

$$\mathscr{C}_{jk} = \frac{3\mathbf{u}_j^{\mathrm{T}}\mathbf{G}_3(\mathbf{u}_k,\mathbf{u}_k,\mathbf{u}_k) + \omega_{0k}^2\mathbf{u}_j^{\mathrm{T}}\mathbf{I}_3(\mathbf{u}_k,\mathbf{u}_k,\mathbf{u}_k) - 3\omega_{0k}^2\mathbf{u}_j^{\mathrm{T}}\mathbf{I}_3^*(\mathbf{u}_k,\mathbf{u}_k,\mathbf{u}_k)}{\omega_{0j}^2 - \omega_{0k}^2} \tag{26}$$

Solving (21) and (23) for $\mathbf{z}_2$ and $\mathbf{w}_2$ yields

$$\mathbf{z}_2 = \sum_{j=1}^{N}\mathscr{D}_{jk}\mathbf{u}_j, \qquad \mathbf{w}_2 = 3\mathrm{i}\omega_{0k}\sum_{j=1}^{N}\mathscr{D}_{jk}\mathbf{u}_j \tag{27}$$

where

$$\mathscr{D}_{jk} = \frac{\mathbf{u}_j^{\mathrm{T}}\mathbf{G}_3(\mathbf{u}_k,\mathbf{u}_k,\mathbf{u}_k) - \omega_{0k}^2\mathbf{u}_j^{\mathrm{T}}\mathbf{I}_3(\mathbf{u}_k,\mathbf{u}_k,\mathbf{u}_k) - \omega_{0k}^2\mathbf{u}_j^{\mathrm{T}}\mathbf{I}_3^*(\mathbf{u}_k,\mathbf{u}_k,\mathbf{u}_k)}{\omega_{0j}^2 - 9\omega_{0k}^2} \tag{28}$$

Finally, substituting (25) and (27) into (18) and (19), the solution of the third-order problem takes the form

$$\mathbf{q}_3 = \left(\frac{\Gamma_{kkk}}{4\omega_{0k}^2}\mathbf{u}_k + \sum_{j=1,j\neq k}^{N}\mathscr{C}_{jk}\mathbf{u}_j\right)\mathrm{e}^{\mathrm{i}\omega_{0k}T_0}A_k^2\overline{A}_k + \left(\sum_{j=1}^{N}\mathscr{D}_{jk}\mathbf{u}_j\right)\mathrm{e}^{3\mathrm{i}\omega_{0k}T_0}A_k^3 + cc \tag{29}$$

$$\mathbf{p}_3 = \mathrm{i}\omega_{0k}\left(-\frac{\Gamma_{kkk}}{4\omega_{0k}^2}\mathbf{u}_k + \sum_{j=1,j\neq k}^{N}\mathscr{C}_{jk}\mathbf{u}_j\right)\mathrm{e}^{\mathrm{i}\omega_{0k}T_0}A_k^2\overline{A}_k + \left(3\mathrm{i}\omega_{0k}\sum_{j=1}^{N}\mathscr{D}_{jk}\mathbf{u}_j\right)\mathrm{e}^{3\mathrm{i}\omega_{0k}T_0}A_k^3 + cc \tag{30}$$

Inserting the polar form for $A_k$, $A_k(T_2) = (1/2)a_k(T_2)\exp(\mathrm{i}\phi(T_2))$, into (16) and separating real and imaginary parts yields

$$D_2 a_k = 0, \qquad D_2\phi_k = -\frac{1}{8\omega_{0k}}\Gamma_{kkk}a_k^2 \tag{31}$$

The first equation expresses the circumstance that the amplitude is constant with respect to the slow scale $T_2$, whilst integrating the latter furnishes the effect of the nonlinearity on the frequency as

$$\phi_k = -\frac{1}{8\omega_{0k}}\Gamma_{kkk}a_k^2\epsilon^2 t + \phi_{0k} \tag{32}$$

where $\phi_{0k}$ is a constant phase depending on the initial conditions.

Substituting (32) into (10), and using the polar form, gives

$$\mathbf{q}_1 = a_k \cos(\omega_k t + \phi_{0k})\mathbf{u}_k = a_k \cos\theta_k \mathbf{u}_k \tag{33}$$

where $\omega_k$ is the nonlinear frequency of the $k$th individual nonlinear normal mode expressed as

$$\omega_k = \omega_{0k} - \alpha_{kkk}\epsilon^2 a_k^2 \tag{34}$$

where $\alpha_{kkk} = \Gamma_{kkk}/(8\omega_{0k})$ is known as the *effective nonlinearity coefficient* and regulates the bending of the *backbone* of the mode (the curve representing the oscillation frequency versus the amplitude). Substituting (29), (30) and (33) into (5) leads to

$$\mathbf{q} = \epsilon a_k \left[\mathbf{u}_k + \epsilon^2 \frac{1}{4} a_k^2 \left( \frac{\Gamma_{kkk}}{4\omega_{0k}^2}\mathbf{u}_k + \sum_{j=1, j\neq k}^{N} \mathscr{C}_{jk}\mathbf{u}_j \right)\right] \cos\theta_k + \epsilon^3 \frac{1}{4} a_k^3 \left( \sum_{j=1}^{N} \mathscr{D}_{jk}\mathbf{u}_j \right) \cos 3\theta_k + \cdots \tag{35}$$

$$\mathbf{p} = -\epsilon\omega_{0k} a_k \left[\mathbf{u}_k + \epsilon^2 \frac{1}{4} a_k^2 \left( -\frac{\Gamma_{kkk}}{4\omega_{0k}^2}\mathbf{u}_k + \sum_{j=1, j\neq k}^{N} \mathscr{C}_{jk}\mathbf{u}_j \right)\right] \sin\theta_k - \epsilon^3 \omega_{0k} \frac{3}{4} a_k^3 \left( \sum_{j=1}^{N} \mathscr{D}_{jk}\mathbf{u}_j \right) \sin 3\theta_k + \cdots \tag{36}$$

Considering that $u_{kj} = \delta_{kj}$, Eqs. (35) and (36) can be rewritten in scalar form as

$$q_k = \epsilon a_k \left( 1 + \frac{1}{16}\frac{\Gamma_{kkk}}{\omega_{0k}^2}\epsilon^2 a_k^2 \right) \cos\theta_k + \frac{1}{4}\epsilon^3 a_k^3 \mathscr{D}_{kk} \cos 3\theta_k + \cdots \tag{37}$$

$$p_k = -\epsilon\omega_{0k} a_k \left( 1 - \frac{1}{16}\frac{\Gamma_{kkk}}{\omega_{0k}^2}\epsilon^2 a_k^2 \right) \sin\theta_k - \frac{3}{4}\epsilon^3 a_k^3 \omega_{0k} \mathscr{D}_{kk} \sin 3\theta_k + \cdots \tag{38}$$

$$q_j = \tfrac{1}{4}\epsilon^3 a_k^3 \left( \mathscr{C}_{jk}\cos\theta_k + \mathscr{D}_{jk}\cos 3\theta_k \right) + \cdots, \quad j \neq k \tag{39}$$

$$p_j = -\omega_{0k}\tfrac{1}{4}\epsilon^3 a_k^3 \left( \mathscr{C}_{jk}\sin\theta_k + 3\mathscr{D}_{jk}\sin 3\theta_k \right) + \cdots, \quad j \neq k \tag{40}$$

The two-dimensional invariant manifold associated with the $k$th individual nonlinear normal mode is found in modal coordinates once the generalized coordinates $q_j$ and $p_j$ are expressed in terms of the 'master' coordinates $q_k$ and $p_k$. The manifold takes the form

$$q_j = \frac{1}{4}\left[ (\mathscr{C}_{jk} + \mathscr{D}_{jk}) q_k^3 + (\mathscr{C}_{jk} - 3\mathscr{D}_{jk}) \frac{q_k p_k^2}{\omega_{0k}^2} \right] + \cdots \tag{41}$$

$$p_j = \frac{1}{4}\left[ (\mathscr{C}_{jk} - 3\mathscr{D}_{jk}) \frac{p_k^3}{\omega_{0k}^2} + (\mathscr{C}_{jk} + 9\mathscr{D}_{jk}) q_k^2 p_k \right] + \cdots \tag{42}$$

To express the manifold in the original physical coordinates instead of the linear modal coordinates, Eqs. (41) and (42) are substituted into the transformations $\mathbf{x} = \mathbf{B}_0\mathbf{q}$ and $\mathbf{y} = \mathbf{B}_0\mathbf{p}$. Consequently,

$$\mathbf{x} \approx q_k \mathbf{b}_{0k} + \sum_{j=1, j\neq k}^{N} \frac{1}{4}\left[ (\mathscr{C}_{jk} + \mathscr{D}_{jk}) q_k^3 + (\mathscr{C}_{jk} - 3\mathscr{D}_{jk}) \frac{q_k p_k^2}{\omega_{0k}^2} \right] \mathbf{b}_{0j} \tag{43}$$

$$\mathbf{y} \approx p_k \mathbf{b}_{0k} + \sum_{j=1, j\neq k}^{N} \frac{1}{4}\left[ (\mathscr{C}_{jk} - 3\mathscr{D}_{jk}) \frac{p_k^3}{\omega_{0k}^2} + (\mathscr{C}_{jk} + 9\mathscr{D}_{jk}) q_k^2 p_k \right] \mathbf{b}_{0j} \tag{44}$$

where $\mathbf{b}_{0j}$ is the $j$th physical linear eigenvector. Letting $q_k(t_0) = a_k$ and $p_k(t_0) = 0$ into (43) and (44), and dividing the result by $a_k$ so as to 'normalize' the shape, the approximate $k$th nonlinear mode shape is obtained in the form

$$\mathbf{b}_k \approx \mathbf{b}_{0k} + a_k^2 \sum_{j=1, j\neq k}^{N} \frac{1}{4}(\mathscr{C}_{jk} + \mathscr{D}_{jk})\mathbf{b}_{0j} \tag{45}$$

Assuming, for sake of conciseness, geometric nonlinearities only (i.e., $\mathbf{I}_3 = \mathbf{I}_3^* = 0$), the closed-form nonlinear mode shape becomes

$$\mathbf{b}_k \approx \mathbf{b}_{0k} + a_k^2 \sum_{j=1, j\neq k}^{N} \left[\frac{1}{4}\left(\frac{3}{\omega_{0j}^2 - \omega_{0k}^2} + \frac{1}{\omega_{0j}^2 - 9\omega_{0k}^2}\right)\mathbf{u}_j^{\mathrm{T}}\mathbf{G}_3(\mathbf{u}_k, \mathbf{u}_k, \mathbf{u}_k)\right]\mathbf{b}_{0j} \tag{46}$$

Inspection of Eq. (46) allows to ascertain that (i) the individual NNM's break down when $\omega_{0j} \approx \omega_{0k}$ (1:1 internal resonance) or $\omega_{0j} \approx 3\omega_{0k}$ (3:1 internal resonance) and (ii) the nonlinear corrections to the $k$th linear mode shape depend quadratically on $a_k$—as in the nonlinear frequency $\omega_k$ in Eq. (34). The strength of the second-order contribution of the $j$th linear mode is regulated by the participation factor enclosed in the square brackets in Eq. (46). This coefficient is proportional to $3(\omega_{0j}^2 - \omega_{0k}^2)^{-1} + (\omega_{0j}^2 - 9\omega_{0k}^2)^{-1}$ and to the virtual work of the nonlinear structural force associated with the $k$th mode in the displacement of the $j$th mode. On the other hand, the leading nonlinear frequency correction term is proportional to $\alpha_{kkk} = 3\mathbf{u}_k^{\mathrm{T}}\mathbf{G}_3(\mathbf{u}_k, \mathbf{u}_k, \mathbf{u}_k)/(8\omega_{0k})$, which, in turn, is proportional to the virtual work of the nonlinear structural force associated with the $k$th mode in the displacement of the $k$th mode itself.

Inspection of Eqs. (43) and (44) allows to draw some general conclusions about the signatures of the individual NNM's. We observe that when $\mathscr{C}_{jk} = \mathscr{D}_{jk} = 0$, for all $j$, then Eqs. (43) and (44) reduce to $\mathbf{x} \approx q_k\mathbf{b}_{0k}$ and $\mathbf{y} \approx p_k\mathbf{b}_{0k}$. Since the resulting dependence of the system phase state on the master coordinates $q_k$ and $p_k$ is linear, these individual NNM's belong to the class of similar nonlinear normal modes (Rosenberg, 1962, 1966).

Considering again, for simplicity, the case of geometric nonlinearities only, the condition for similar normal modes, i.e., $\mathscr{C}_{jk} = \mathscr{D}_{jk} = 0$, implies $\mathbf{u}_j^{\mathrm{T}}\mathbf{G}_3(\mathbf{u}_k, \mathbf{u}_k, \mathbf{u}_k) = 0$. This condition possesses a clear mechanical meaning: *the leading nonlinear structural force associated with the kth mode does not perform work in the virtual displacement of the jth mode, for all $j \neq k$*. Therefore, there cannot be corrections from the other modes to the $k$th linear normal mode.

It is useful to see how to exploit the presented results when dealing with spatially continuous systems. Employing the discretization approach, the distributed-parameter system is transformed into a discrete system. Following the same line of analysis used for discrete structural systems, one viable strategy is to seek the nonlinear normal modes as a superposition of the linear normal modes $\Phi_j(x)$ as

$$v(x,t) \approx \sum_{j=1}^{N} q_j(t)\Phi_j(x) \tag{47}$$

where $v(x,t)$ is the unknown displacement, $q_j$ is the linear modal coordinate and $N$ is the number of linear modes retained in the discretization process. Then, using, e.g., the Galerkin method to minimize the residuals, the discretized equations in the modal coordinates are obtained in the form of Eq. (2). Thereafter, assuming as initial conditions $q_k(t_0) = a_k$, $p_k(t_0) = 0$, and substituting (41) and (42) into (47), the $k$th nonlinear mode shape can be expressed as $v_k(x,t_0) \approx a_k\Phi_k(x) + 1/4a_k^3\sum_{j=1,j\neq k}^{N}(\mathscr{C}_{jk} + \mathscr{D}_{jk})\Phi_j(x)$. Next, dividing the obtained function by $a_k$, so as to normalize the mode shape with respect to $a_k$, yields the following nonlinear mode shape:

$$\Psi_k(x) \approx \Phi_k(x) + a_k^2 \sum_{j=1, j\neq k}^{N} \frac{1}{4}\left(\mathscr{C}_{jk} + \mathscr{D}_{jk}\right)\Phi_j(x) \tag{48}$$

## 4. Resonant nonlinear normal modes

When two or more frequencies are commensurable with an appropriate integer ratio, the structure may experience internal resonances. When such a condition occurs, an energy exchange between the two (or more) resonant modes is observed. Hence, the general solution presented in the previous section must be modified in order to account for the modal interaction.

Assuming that two arbitrary frequencies, $\omega_{0m}$ and $\omega_{0n}$, are commensurable, the first-order solution of (7) is replaced by

$$\mathbf{q}_1 = A_m \mathrm{e}^{\mathrm{i}\omega_{0m}T_0}\mathbf{u}_m + A_n \mathrm{e}^{\mathrm{i}\omega_{0n}T_0}\mathbf{u}_n + cc \tag{49}$$

$$\mathbf{p}_1 = \mathrm{i}\omega_{0m} A_m \mathrm{e}^{\mathrm{i}\omega_{0m}T_0}\mathbf{u}_m + \mathrm{i}\omega_{0n} A_n \mathrm{e}^{\mathrm{i}\omega_{0n}T_0}\mathbf{u}_n + cc \tag{50}$$

Since the problem at order $\epsilon^2$ is empty as shown in Section 3, $A_m = A_m(T_2)$ and $A_n = A_n(T_2)$. Equations (49) and (50) are substituted into the third-order problem which, in turn, becomes

$$D_0\mathbf{q}_3 - \mathbf{p}_3 = -(D_2 A_m)\mathrm{e}^{\mathrm{i}\omega_{0m}T_0}\mathbf{u}_m - (D_2 A_n)\mathrm{e}^{\mathrm{i}\omega_{0n}T_0}\mathbf{u}_n + cc \tag{51}$$

$$\begin{aligned} D_0\mathbf{p}_3 + \mathbf{\Lambda}\mathbf{q}_3 = {} & -\mathrm{i}\omega_{0m}(D_2 A_m)\mathrm{e}^{\mathrm{i}\omega_{0m}T_0}\mathbf{u}_m - \mathrm{i}\omega_{0n}(D_2 A_n)\mathrm{e}^{\mathrm{i}\omega_{0n}T_0}\mathbf{u}_n + \sum_{k=m,n}\mathbf{a}_{kkk}A_k^2\overline{A}_k\mathrm{e}^{\mathrm{i}\omega_{0k}T_0} \\ & + \sum_{k=m,n}\mathbf{b}_{kkk}A_k^3\mathrm{e}^{3\mathrm{i}\omega_{0k}T_0} + \mathbf{R}_{mn}A_m A_n\overline{A}_n\mathrm{e}^{\mathrm{i}\omega_{0m}T_0} + \mathbf{R}_{nm}A_n A_m\overline{A}_m\mathrm{e}^{\mathrm{i}\omega_{0n}T_0} + \mathbf{S}_{mn}A_n\overline{A}_m^2\mathrm{e}^{\mathrm{i}(\omega_{0n}-2\omega_{0m})T_0} \\ & + \mathbf{S}_{nm}A_n^2\overline{A}_m\mathrm{e}^{\mathrm{i}(2\omega_{0n}-\omega_{0m})T_0} + cc \end{aligned} \tag{52}$$

where

$$\mathbf{a}_{kkk} = 3\mathbf{G}_3(\mathbf{u}_k,\mathbf{u}_k,\mathbf{u}_k) + \omega_{0k}^2\mathbf{I}_3(\mathbf{u}_k,\mathbf{u}_k,\mathbf{u}_k) - 3\omega_{0k}^2\mathbf{I}_3^*(\mathbf{u}_k,\mathbf{u}_k,\mathbf{u}_k) \tag{53}$$

$$\mathbf{b}_{kkk} = \mathbf{G}_3(\mathbf{u}_k,\mathbf{u}_k,\mathbf{u}_k) - \omega_{0k}^2\mathbf{I}_3(\mathbf{u}_k,\mathbf{u}_k,\mathbf{u}_k) - \omega_{0k}^2\mathbf{I}_3^*(\mathbf{u}_k,\mathbf{u}_k,\mathbf{u}_k) \tag{54}$$

$$\begin{aligned} \mathbf{R}_{mn} = {} & 2\mathbf{G}_3(\mathbf{u}_m,\mathbf{u}_n,\mathbf{u}_n) + 2\mathbf{G}_3(\mathbf{u}_n,\mathbf{u}_m,\mathbf{u}_n) + 2\mathbf{G}_3(\mathbf{u}_n,\mathbf{u}_n,\mathbf{u}_m) + 2\omega_{0n}^2\mathbf{I}_3(\mathbf{u}_m,\mathbf{u}_n,\mathbf{u}_n) - 2\omega_{0n}^2\mathbf{I}_3^*(\mathbf{u}_m,\mathbf{u}_n,\mathbf{u}_n) \\ & - 2\omega_{0m}^2\mathbf{I}_3^*(\mathbf{u}_n,\mathbf{u}_n,\mathbf{u}_m) - 2\omega_{0n}^2\mathbf{I}_3^*(\mathbf{u}_n,\mathbf{u}_m,\mathbf{u}_n) \end{aligned} \tag{55}$$

$$\begin{aligned} \mathbf{R}_{nm} = {} & 2\mathbf{G}_3(\mathbf{u}_n,\mathbf{u}_m,\mathbf{u}_m) + 2\mathbf{G}_3(\mathbf{u}_m,\mathbf{u}_n,\mathbf{u}_m) + 2\mathbf{G}_3(\mathbf{u}_m,\mathbf{u}_m,\mathbf{u}_n) + 2\omega_{0m}^2\mathbf{I}_3(\mathbf{u}_n,\mathbf{u}_m,\mathbf{u}_m) \\ & - 2\omega_{0m}^2\mathbf{I}_3^*(\mathbf{u}_n,\mathbf{u}_m,\mathbf{u}_m) - 2\omega_{0n}^2\mathbf{I}_3^*(\mathbf{u}_m,\mathbf{u}_m,\mathbf{u}_n) - 2\omega_{0m}^2\mathbf{I}_3^*(\mathbf{u}_m,\mathbf{u}_n,\mathbf{u}_m) \end{aligned} \tag{56}$$

$$\begin{aligned} \mathbf{S}_{mn} = {} & \mathbf{G}_3(\mathbf{u}_m,\mathbf{u}_m,\mathbf{u}_n) - \omega_{0m}^2\mathbf{I}_3(\mathbf{u}_n,\mathbf{u}_m,\mathbf{u}_m) + \omega_{0n}\omega_{0m}(\mathbf{I}_3(\mathbf{u}_m,\mathbf{u}_n,\mathbf{u}_m) + \mathbf{I}_3(\mathbf{u}_m,\mathbf{u}_m,\mathbf{u}_n)) \\ & - \omega_{0m}^2\mathbf{I}_3^*(\mathbf{u}_n,\mathbf{u}_m,\mathbf{u}_m) - \omega_{0n}^2\mathbf{I}_3^*(\mathbf{u}_m,\mathbf{u}_m,\mathbf{u}_n) - \omega_{0m}^2\mathbf{I}_3^*(\mathbf{u}_m,\mathbf{u}_n,\mathbf{u}_m) \end{aligned} \tag{57}$$

$$\begin{aligned} \mathbf{S}_{nm} = {} & \mathbf{G}_3(\mathbf{u}_n,\mathbf{u}_n,\mathbf{u}_m) - \omega_{0n}^2\mathbf{I}_3(\mathbf{u}_m,\mathbf{u}_n,\mathbf{u}_n) + \omega_{0n}\omega_{0m}(\mathbf{I}_3(\mathbf{u}_n,\mathbf{u}_m,\mathbf{u}_n) + \mathbf{I}_3(\mathbf{u}_n,\mathbf{u}_n,\mathbf{u}_m)) \\ & - \omega_{0n}^2(\mathbf{I}_3^*(\mathbf{u}_m,\mathbf{u}_n,\mathbf{u}_n) + \mathbf{I}_3^*(\mathbf{u}_n,\mathbf{u}_m,\mathbf{u}_n)) - \omega_{0m}^2\mathbf{I}_3^*(\mathbf{u}_n,\mathbf{u}_n,\mathbf{u}_m) \end{aligned} \tag{58}$$

In the following, a typical internal resonance for systems with cubic nonlinearities is considered, namely, a three-to-one internal resonance. To describe quantitatively the nearness of $\omega_{0m}$ and $\omega_{0n}$, the detuning parameter $\sigma$ is introduced as

$$\omega_{0n} = 3\omega_{0m} + \epsilon^2\sigma \tag{59}$$

Imposing separately the two orthogonality conditions between the solutions of the adjoint homogeneous problem and the inhomogeneous terms of (51) and (52), the following modulation equations are obtained:

$$D_2A_m = \frac{1}{2\mathrm{i}\omega_{0m}}\left[\boldsymbol{\Gamma}_{mmm}A_m^2\overline{A}_m + (\mathbf{u}_m^{\mathrm{T}}\mathbf{R}_{mn})A_mA_n\overline{A}_n + (\mathbf{u}_m^{\mathrm{T}}\mathbf{S}_{mn})A_n\overline{A}_m^2\mathrm{e}^{\mathrm{i}\sigma T_2}\right] \tag{60}$$

$$D_2A_n = \frac{1}{2\mathrm{i}\omega_{0n}}\left[\boldsymbol{\Gamma}_{nnn}A_n^2\overline{A}_n + (\mathbf{u}_n^{\mathrm{T}}\mathbf{R}_{nm})A_nA_m\overline{A}_m + (\mathbf{u}_n^{\mathrm{T}}\mathbf{b}_{mmm})A_m^3\mathrm{e}^{-\mathrm{i}\sigma T_2}\right] \tag{61}$$

where $\Gamma_{jjj} = \mathbf{u}_j^{\mathrm{T}}\mathbf{a}_{jjj}$, with $j = m, n$, and is explicitly given by Eq. (17).

Substituting (60) and (61) into (51) and (52), the solution at order $\epsilon^3$ is sought in the form

$$\begin{aligned}\mathbf{q}_3 = {} & \mathbf{z}_1A_mA_n\overline{A}_n\mathrm{e}^{\mathrm{i}\omega_{0m}T_0} + \mathbf{z}_2A_nA_m\overline{A}_m\mathrm{e}^{\mathrm{i}\omega_{0n}T_0} + \mathbf{z}_3A_m^2\overline{A}_m\mathrm{e}^{\mathrm{i}\omega_{0m}T_0} + \mathbf{z}_4A_n^2\overline{A}_n\mathrm{e}^{\mathrm{i}\omega_{0n}T_0} + \mathbf{z}_5A_n\overline{A}_m^2\mathrm{e}^{\mathrm{i}(\omega_{0n}-2\omega_{0m})T_0} \\ & + \mathbf{z}_6A_n^2\overline{A}_m\mathrm{e}^{\mathrm{i}(2\omega_{0n}-\omega_{0m})T_0} + \mathbf{z}_7A_m^3\mathrm{e}^{3\mathrm{i}\omega_{0m}T_0} + \mathbf{z}_8A_n^3\mathrm{e}^{3\mathrm{i}\omega_{0n}T_0} + cc\end{aligned} \tag{62}$$

$$\begin{aligned}\mathbf{p}_3 = i\Big[ & \tilde{\mathbf{w}}_1A_mA_n\overline{A}_n\mathrm{e}^{\mathrm{i}\omega_{0m}T_0} + \tilde{\mathbf{w}}_2A_nA_m\overline{A}_m\mathrm{e}^{\mathrm{i}\omega_{0n}T_0} + \tilde{\mathbf{w}}_3A_m^2\overline{A}_m\mathrm{e}^{\mathrm{i}\omega_{0m}T_0} + \tilde{\mathbf{w}}_4A_n^2\overline{A}_n\mathrm{e}^{\mathrm{i}\omega_{0n}T_0} + \tilde{\mathbf{w}}_5A_n\overline{A}_m^2\mathrm{e}^{\mathrm{i}(\omega_{0n}-2\omega_{0m})T_0} \\ & + \tilde{\mathbf{w}}_6A_n^2\overline{A}_m\mathrm{e}^{\mathrm{i}(2\omega_{0n}-\omega_{0m})T_0} + \tilde{\mathbf{w}}_7A_m^3\mathrm{e}^{3\mathrm{i}\omega_{0m}T_0} + \tilde{\mathbf{w}}_8A_n^3\mathrm{e}^{3\mathrm{i}\omega_{0n}T_0}\Big] + cc\end{aligned} \tag{63}$$

Inserting (62) and (63) into (51) and (52), and equating the coefficients of like harmonic terms to 0, a set of 16 algebraic problems is obtained as reported, along with the solutions, in Appendix A.

Expressing $A_m$ and $A_n$ in polar forms

$$A_m(T_2) = \tfrac{1}{2}a_m(T_2)\mathrm{e}^{\mathrm{i}\phi_m(T_2)} \quad \text{and} \quad A_n(T_2) = \tfrac{1}{2}a_n(T_2)\mathrm{e}^{\mathrm{i}\phi_n(T_2)} \tag{64}$$

and substituting them into the modulation equations (60) and (61), and separating real and imaginary parts, yields

$$D_2a_m = \frac{(\mathbf{u}_m^{\mathrm{T}}\mathbf{S}_{mn})}{8\omega_{0m}}a_na_m^2\sin\gamma \tag{65}$$

$$D_2a_n = -\frac{(\mathbf{u}_n^{\mathrm{T}}\mathbf{b}_{mmm})}{8\omega_{0n}}a_m^3\sin\gamma \tag{66}$$

$$a_mD_2\phi_m = -\frac{\Gamma_{mmm}}{8\omega_{0m}}a_m^3 - \frac{(\mathbf{u}_m^{\mathrm{T}}\mathbf{R}_{mn})}{8\omega_{0m}}a_n^2a_m - \frac{(\mathbf{u}_m^{\mathrm{T}}\mathbf{S}_{mn})}{8\omega_{0m}}a_na_m^2\cos\gamma \tag{67}$$

$$a_nD_2\phi_n = -\frac{\Gamma_{nnn}}{8\omega_{0n}}a_n^3 - \frac{(\mathbf{u}_n^{\mathrm{T}}\mathbf{R}_{nm})}{8\omega_{0n}}a_m^2a_n - \frac{(\mathbf{u}_n^{\mathrm{T}}\mathbf{b}_{mmm})}{8\omega_{0n}}a_m^3\cos\gamma \tag{68}$$

where $\gamma = \sigma T_2 + \phi_n - 3\phi_m$ is the relative phase.

The modulation equations (60) and (61), cast in Cartesian form, can describe a wide range of motions, including also quasiperiodic and chaotic motions. Here, we are specifically interested in periodic motions whereby the nonlinear frequencies of the interacting modes lock into an integer ratio equal to 3. The local bifurcations of these motions indicate the post-critical responses bifurcating from them although these do not cover the full range of solutions which could be captured by a global analysis only. Moreover, the periodic motions provide an underlying 'skeleton' structure to the system behavior also in the presence of weak damping and forcing.

Seeking periodic structural motions, $a_m$ and $a_n$ must be constant; hence, $D_2a_m = D_2a_n = 0$ and Eqs. (65) and (66) are satisfied when (a) $a_m = 0$ and $a_n \neq 0$ and (b) $(a_m, a_n) \neq (0, 0)$ and $\sin\gamma = 0$ because $(\mathbf{u}_m^{\mathrm{T}}\mathbf{S}_{mn})$ and $(\mathbf{u}_n^{\mathrm{T}}\mathbf{b}_{mmm})$ are assumed different from 0. The first case corresponds to the uncoupled high-frequency mode whereas case (b) yields coupled modes. For coupled modes, $\gamma = k\pi$, with $k = 0, \pm1, \pm2, \ldots$ The third independent equation governs the modulation of the relative phase and is obtained as

$$D_2\gamma = \sigma + D_2\phi_n - 3D_2\phi_m \tag{69}$$

Dividing (67) and (68) by $a_m$ and $a_n$, respectively, and substituting the resulting expressions into (69), and letting $D_2\gamma = 0$, leads to

$$\begin{aligned} D_2\gamma = {} & \left[\frac{3\Gamma_{mmm}}{8\omega_{0m}} - \frac{(\mathbf{u}_n^{\mathrm{T}}\mathbf{R}_{nm})}{8\omega_{0n}}\right]a_m^2 + \left[\frac{(3\mathbf{u}_m^{\mathrm{T}}\mathbf{R}_{mn})}{8\omega_{0m}} - \frac{\Gamma_{nnn}}{8\omega_{0n}}\right]a_n^2 + \frac{(3\mathbf{u}_m^{\mathrm{T}}\mathbf{S}_{mn})}{8\omega_{0m}}(\cos\gamma)a_n a_m \\ & - \frac{(\mathbf{u}_n^{\mathrm{T}}\mathbf{b}_{mmm})}{8\omega_{0n}}(\cos\gamma)\frac{a_m^3}{a_n} + \sigma = 0 \end{aligned} \tag{70}$$

Dividing (70) by $a_n^2$, the following equation is obtained:

$$\frac{(\mathbf{u}_n^{\mathrm{T}}\mathbf{b}_{mmm})}{8\omega_{0n}}(\cos\gamma)c^3 + \left[\frac{(\mathbf{u}_n^{\mathrm{T}}\mathbf{R}_{nm})}{8\omega_{0n}} - \frac{3\Gamma_{mmm}}{8\omega_{0m}}\right]c^2 - \frac{(3\mathbf{u}_m^{\mathrm{T}}\mathbf{S}_{mn})}{8\omega_{0m}}(\cos\gamma)c + \left[\frac{\Gamma_{nnn}}{8\omega_{0n}} - \frac{(3\mathbf{u}_m^{\mathrm{T}}\mathbf{R}_{mn})}{8\omega_{0m}}\right] - \sigma^* = 0 \tag{71}$$

where $c = a_m/a_n$ and $\sigma^* = \sigma/a_n^2$. Since it is $\gamma = k\pi$, $\cos\gamma = \pm1$; however, as shown in (Lacarbonara et al., 2003) equations of type (71), with $\gamma = k\pi$, possess at most three solutions. Therein, it is also demonstrated that if

$$\mathbf{u}_n^{\mathrm{T}}\mathbf{b}_{mmm} = 0 \tag{72}$$

the two modes under investigation are orthogonal and, hence, they do not interact.

Among all of the solutions of (71), one needs to distinguish those that are stable from those that are unstable. This can be achieved calculating the eigenvalues of the following Jacobian matrix:

$$J(a_m, a_n, \gamma) = \begin{bmatrix} \frac{\partial(D_2a_m)}{\partial a_m} & \frac{\partial(D_2a_m)}{\partial a_n} & \frac{\partial(D_2a_m)}{\partial\gamma} \\ \frac{\partial(D_2a_n)}{\partial a_m} & \frac{\partial(D_2a_n)}{\partial a_n} & \frac{\partial(D_2a_n)}{\partial\gamma} \\ \frac{\partial(D_2\gamma)}{\partial a_m} & \frac{\partial(D_2\gamma)}{\partial a_n} & \frac{\partial(D_2\gamma)}{\partial\gamma} \end{bmatrix} \tag{73}$$

Using Eqs. (65), (66) and (70), Eq. (73) becomes

$$J = \begin{bmatrix} 0 & 0 & \chi_1 \\ 0 & 0 & \chi_2 \\ \chi_3 & \chi_4 & 0 \end{bmatrix} \tag{74}$$

where

$$\begin{aligned} \chi_1 &= \frac{(\mathbf{u}_m^{\mathrm{T}}\mathbf{S}_{mn})}{8\omega_{0m}}a_n a_m^2, \quad \chi_2 = -\frac{(\mathbf{u}_n^{\mathrm{T}}\mathbf{b}_{mmm})}{8\omega_{0n}}a_m^3, \\ \chi_3 &= 2\left[\frac{3\Gamma_{mmm}}{8\omega_{0m}} - \frac{(\mathbf{u}_n^{\mathrm{T}}\mathbf{R}_{nm})}{8\omega_{0n}}\right]a_m + \frac{(3\mathbf{u}_m^{\mathrm{T}}\mathbf{S}_{mn})}{8\omega_{0m}}a_n - 3\frac{(\mathbf{u}_n^{\mathrm{T}}\mathbf{b}_{mmm})}{8\omega_{0n}}\frac{a_m^2}{a_n}, \\ \chi_4 &= 2\left[\frac{(3\mathbf{u}_m^{\mathrm{T}}\mathbf{R}_{mn})}{8\omega_{0m}} - \frac{\Gamma_{nnn}}{8\omega_{0n}}\right]a_n + \frac{(3\mathbf{u}_m^{\mathrm{T}}\mathbf{S}_{mn})}{8\omega_{0m}}a_m + \frac{(\mathbf{u}_n^{\mathrm{T}}\mathbf{b}_{mmm})}{8\omega_{0n}}\frac{a_m^3}{a_n^2} \end{aligned}$$

The eigenvalues of (74), on account of the fact that the first- and third-order invariants of the Jacobian matrix (74) are 0, are expressed as

$$\lambda_1 = 0, \qquad \lambda_{2,3} = \pm\sqrt{-I_2} \tag{75}$$

where $I_2 = -(\chi_2\chi_4 + \chi_3\chi_1)$ is the second-order invariant. In order to have marginally stable solutions, $\lambda_{2,3}$ must be imaginary, that is, $I_2 > 0$, equivalently $(\chi_2\chi_4 + \chi_3\chi_1) < 0$. Consequently, the modes are unstable when $I_2 < 0$, that is $(\chi_2\chi_4 + \chi_3\chi_1) > 0$. This condition can be rewritten as

$$\left(\frac{\mathbf{u}_n^{\mathrm{T}}\mathbf{b}_{mmm}}{8\omega_{0n}}\right)^2 c^4 + 2\left(\frac{\mathbf{u}_n^{\mathrm{T}}\mathbf{b}_{mmm}}{8\omega_{0n}}\right)\left(\frac{3\mathbf{u}_m^{\mathrm{T}}\mathbf{S}_{mn}}{8\omega_{0m}}\right)c^2 + 2\left[\left(\frac{\mathbf{u}_n^{\mathrm{T}}\mathbf{b}_{mmm}}{8\omega_{0n}}\right)\left(\frac{3\mathbf{u}_m^{\mathrm{T}}\mathbf{R}_{mn}}{8\omega_{0m}} - \frac{\Gamma_{nnn}}{8\omega_{0n}}\right)\right.$$
$$\left. - \left(\frac{\mathbf{u}_m^{\mathrm{T}}\mathbf{S}_{mn}}{8\omega_{0m}}\right)\left(\frac{3\Gamma_{mmm}}{8\omega_{0m}} - \frac{\mathbf{u}_n^{\mathrm{T}}\mathbf{R}_{nm}}{8\omega_{0n}}\right)\right]c - \left(\frac{\mathbf{u}_m^{\mathrm{T}}\mathbf{S}_{mn}}{8\omega_{0m}}\right)\left(\frac{3\mathbf{u}_m^{\mathrm{T}}\mathbf{S}_{mn}}{8\omega_{0m}}\right) < 0 \tag{76}$$

Solving the inequality (76) gives the range of $c$ where the solution becomes unstable.

Next, the displacement and velocity vectors are cast in real form. Integrating (67) and (68), the phases $\phi_m$ and $\phi_n$ are obtained as

$$\phi_m = -\frac{1}{8\omega_{0m}}\epsilon^2\left[\Gamma_{mmm}a_m^2 + \left(\mathbf{u}_m^{\mathrm{T}}\mathbf{R}_{mn}\right)a_n^2 + \left(\mathbf{u}_m^{\mathrm{T}}\mathbf{S}_{mn}\right)a_n a_m(\cos\gamma)\right]t + \phi_{0m} \tag{77}$$

$$\phi_n = -\frac{1}{8\omega_{0n}}\epsilon^2\left[\Gamma_{nnn}a_n^2 + \left(\mathbf{u}_n^{\mathrm{T}}\mathbf{R}_{nm}\right)a_m^2 + \left(\mathbf{u}_n^{\mathrm{T}}\mathbf{b}_{mmm}\right)\frac{a_m^3}{a_n}(\cos\gamma)\right]t + \phi_{0n} \tag{78}$$

where $\phi_{0m}$ and $\phi_{0n}$ are constant phases which depend on the initial conditions.

Substituting (77) and (78) into (64) and then into (49) and (50) yields

$$\mathbf{q}_1 = a_m\cos\theta_m\mathbf{u}_m + a_n\cos\theta_n\mathbf{u}_n, \qquad \mathbf{p}_1 = -\omega_{0m}a_m\sin\theta_m\mathbf{u}_m - \omega_{0n}a_n\sin\theta_n\mathbf{u}_n \tag{79}$$

where $\theta_k = \omega_k t + \phi_{0k}$, with $k = m, n$, and the nonlinear frequencies are expressed as

$$\omega_m = \omega_{0m} - \frac{1}{8\omega_{0m}}\epsilon^2 a_n^2\left[\Gamma_{mmm}c^2 + \left(\mathbf{u}_m^{\mathrm{T}}\mathbf{S}_{mn}\right)(\cos\gamma)c + \left(\mathbf{u}_m^{\mathrm{T}}\mathbf{R}_{mn}\right)\right] + \cdots \tag{80}$$

$$\omega_n = 3\omega_{0m} + \epsilon^2 a_n^2\left\{\sigma^* - \frac{1}{8\omega_{0n}}\left[\left(\mathbf{u}_n^{\mathrm{T}}\mathbf{b}_{mmm}\right)(\cos\gamma)c^3 + \left(\mathbf{u}_n^{\mathrm{T}}\mathbf{R}_{nm}\right)c^2 + \Gamma_{nnn}\right]\right\} + \cdots \tag{81}$$

where $c = a_m/a_n$. Substituting the normalized detuning $\sigma^*$ given by Eq. (71) into (81), it can be shown that $\omega_n = 3\omega_m$. That is, the nonlinear resonance tunes the phases of the modes so as to render the ratio between the nonlinear frequencies exactly equal to 3.

Substituting (77) and (78) into (64) and then into (49) and (50), using (5) and (79) yields

$$\mathbf{q} \approx a_m\cos\theta_m\mathbf{u}_m + a_n\cos\theta_n\mathbf{u}_n + \tfrac{1}{4}(\mathbf{z}_1a_n^2 + \mathbf{z}_3a_m^2)a_m\cos\theta_m + \tfrac{1}{4}(\mathbf{z}_2a_m^2 + \mathbf{z}_4a_n^2)a_n\cos(3\theta_m + \gamma)$$
$$+ \tfrac{1}{4}\mathbf{z}_5a_m^2a_n\cos(\theta_m + \gamma) + \tfrac{1}{4}\mathbf{z}_6a_ma_n^2\cos(5\theta_m + 2\gamma) + \tfrac{1}{4}\mathbf{z}_7a_m^3\cos 3\theta_m + \tfrac{1}{4}\mathbf{z}_8a_n^3\cos(9\theta_m + 3\gamma) \tag{82}$$

$$\mathbf{p} \approx -\omega_{0m}a_m\sin\theta_m\mathbf{u}_m - \omega_{0n}a_n\sin\theta_n\mathbf{u}_n - \tfrac{1}{4}(\tilde{\mathbf{w}}_1a_n^2 + \tilde{\mathbf{w}}_3a_m^2)a_m\sin\theta_m - \tfrac{1}{4}(\tilde{\mathbf{w}}_2a_m^2 + \tilde{\mathbf{w}}_4a_n^2)a_n\sin(3\theta_m + \gamma)$$
$$- \tfrac{1}{4}\tilde{\mathbf{w}}_5a_m^2a_n\sin(\theta_m + \gamma) - \tfrac{1}{4}\tilde{\mathbf{w}}_6a_ma_n^2\sin(5\theta_m + 2\gamma) - \tfrac{1}{4}\tilde{\mathbf{w}}_7a_m^3\sin 3\theta_m - \tfrac{1}{4}\tilde{\mathbf{w}}_8a_n^3\sin(9\theta_m + 3\gamma) \tag{83}$$

From Eqs. (82) and (83), the $m$th, $n$th and $j$th components of $\mathbf{q}$ and $\mathbf{p}$ can be explicitly written as

$$q_m = \epsilon a_m\cos\theta_m + \cdots, \qquad p_m = -\epsilon\omega_{0m}a_m\sin\theta_m + \cdots \tag{84}$$

$$q_n = \epsilon a_n\cos(3\theta_m + \gamma) + \cdots, \qquad p_n = -\epsilon\omega_{0n}a_n\sin(3\theta_m + \gamma) + \cdots \tag{85}$$

$$q_j = \epsilon^3\big[(r_{1j}a_n^2 + r_{3j}a_m^2)a_m\cos\theta_m + (r_{2j}a_m^2 + r_{4j}a_n^2)a_n\cos(3\theta_m+\gamma) + r_{5j}a_m^2a_n\cos(\theta_m+\gamma) + r_{6j}a_n^2a_m\cos(5\theta_m+2\gamma) + r_{7j}a_m^3\cos 3\theta_m + r_{8j}a_n^3\cos(9\theta_m+3\gamma)\big] + \cdots \tag{86}$$

$$p_j = \epsilon^3\big[(s_{1j}a_n^2 + s_{3j}a_m^2)a_m\sin\theta_m + (s_{2j}a_m^2 + s_{4j}a_n^2)a_n\sin(3\theta_m+\gamma) + s_{5j}a_m^2a_n\sin(\theta_m+\gamma) + s_{6j}a_n^2a_m\sin(5\theta_m+2\gamma) + s_{7j}a_m^3\sin 3\theta_m + s_{8j}a_n^3\sin(9\theta_m+3\gamma)\big] + \cdots \tag{87}$$

where the coefficients $r_{ij}$ and $s_{ij}$, $i = 1\cdots 8$, are reported in Appendix A.

Using Eqs. (84)–(87) and trigonometric identities to express $q_j$ and $p_j$ in terms of $q_m$, $q_n$, $p_m$, and $p_n$, the four-dimensional invariant manifold of the two resonant nonlinear normal modes is obtained as:

$$q_j = \alpha_{1j}p_m^2q_m + \alpha_{2j}q_mp_mp_n + \alpha_{3j}p_n^2q_m + \alpha_{mj}q_m^3 + \alpha_{5j}q_np_m^2 + \alpha_{6j}q_np_mp_n + \alpha_{7j}p_n^2q_n + \alpha_{nj}q_n^3 + \cdots \tag{88}$$

$$p_j = \beta_{mj}p_m^3 + \beta_{2j}p_m^2p_n + \beta_{3j}p_mp_n^2 + \beta_{nj}p_n^3 + \beta_{5j}q_m^2p_m + \beta_{6j}q_mq_np_m + \beta_{7j}q_mq_np_n + \beta_{8j}p_nq_n^2 + \cdots \tag{89}$$

where the coefficients $\alpha_{ij}$ and $\beta_{ij}$, $i = 1\cdots 8$, are reported in Appendix A.

Next, the manifold is expressed in the physical coordinate space substituting Eqs. (88) and (89) into the transformations $\mathbf{x} = \mathbf{B}_0\mathbf{q}$ and $\mathbf{y} = \mathbf{B}_0\mathbf{p}$ thereby obtaining

$$\mathbf{x} \approx (q_m\mathbf{b}_{0m} + q_n\mathbf{b}_{0n}) + \sum_{j=1, j\neq m,n}^{N}\big[\alpha_{1j}p_m^2q_m + \alpha_{2j}q_mp_mp_n + \alpha_{3j}p_n^2q_m + \alpha_{mj}q_m^3 + \alpha_{5j}q_np_m^2 + \alpha_{6j}q_np_mp_n + \alpha_{7j}p_n^2q_n + \alpha_{nj}q_n^3\big]\mathbf{b}_{0j} \tag{90}$$

$$\mathbf{y} \approx (p_m\mathbf{b}_{0m} + p_n\mathbf{b}_{0n}) + \sum_{j=1, j\neq m,n}^{N}\big[\beta_{mj}p_m^3 + \beta_{2j}p_m^2p_n + \beta_{3j}p_mp_n^2 + \beta_{nj}p_n^3 + \beta_{5j}q_m^2p_m + \beta_{6j}q_mq_np_m + \beta_{7j}q_mq_np_n + \beta_{8j}p_nq_n^2\big]\mathbf{b}_{0j} \tag{91}$$

Then, the nonlinear resonant mode shapes can be obtained putting $q_m(t_0) = a_m$, $q_n(t_0) = a_n$ and $p_m(t_0) = p_n(t_0) = 0$ into Eqs. (90) and (91). The resulting nonlinear modes can be normalized with respect to the amplitude of the high-frequency mode, $a_n$. Therefore,

$$\mathbf{b}_{mn} \approx (c\mathbf{b}_{0m} + \mathbf{b}_{0n}) + a_n^2\sum_{j=1, j\neq m,n}^{N}\big[c^3\alpha_{mj} + \alpha_{nj}\big]\mathbf{b}_{0j} \tag{92}$$

where $\mathbf{b}_{mn} = \mathbf{x}/a_n$ and $\mathbf{y} = \mathbf{0}$.

Considering a distributed-parameter system and employing the discretization approach, the resonant NNM's can be obtained substituting (88) and (89) into (47). Dividing the result by $a_n$ yields the normalized resonant nonlinear mode shapes in the form

$$\Psi_{mn}(x) = c\Phi_m(x) + \Phi_n(x) + a_n^2\sum_{j=1, j\neq m, j\neq n}^{N}\frac{1}{4}\left\{c^3\left[\frac{\mathbf{u}_j^{\mathrm{T}}\mathbf{a}_{mmm}}{\omega_{0j}^2-\omega_{0m}^2} + \frac{\mathbf{u}_j^{\mathrm{T}}\mathbf{b}_{mmm}}{(\omega_{0j}^2-9\omega_{0m}^2)}\right] + \left[\frac{\mathbf{u}_j^{\mathrm{T}}\mathbf{a}_{nnn}}{\omega_{0j}^2-\omega_{0n}^2} + \frac{\mathbf{u}_j^{\mathrm{T}}\mathbf{b}_{nnn}}{\omega_{0j}^2-9\omega_{0n}^2}\right]\right\}\Phi_j(x) \tag{93}$$

where the bracketed expression is the extended form of $(c^3\alpha_{mj} + \alpha_{nj})$.

## 5. Illustrative example

In this section, the general theoretical results are applied to an illustrative example: a hinged–hinged uniform, linearly elastic, beam with a lumped mass $m$ rigidly attached at an arbitrary location denoted with $x_1^*$ (the star indicates dimensional variables). The geometry of the beam is pictured in Fig. 1. It is supposed that (i) the beam oscillates in the initial rest plane with moderately large transverse deflections (shallow configurations); (ii) the constraints act as perfect fixed hinges; (iii) Euler–Bernoulli linear bending theory holds; (iv) no initial conditions are prescribed in the longitudinal direction. As a result of assumptions (i) and (iv), the axial strain $\epsilon_0$ of the beam centerline due to the transverse displacement $v$ is constant along the beam span and is computed as follows (Mettler, 1962):

$$\epsilon_0 = \frac{1}{2\ell}\int_0^\ell (v^{*'})^2 \, \mathrm{d}x^* \tag{94}$$

where $\ell$ is the beam undeformed length and the prime indicates differentiation with respect to the coordinate $x^*$.

The beam elastic potential energy is given by both the bending and axial deformation energies and can be written as

$$V[v^*(x^*, t^*)] = \frac{1}{2}\int_0^\ell EI(v^{*''})^2 \, \mathrm{d}x^* + \frac{1}{8l^2}\int_0^\ell EA\left(\int_0^\ell \left(v^{*'}\right)^2 \mathrm{d}x^*\right)^2 \mathrm{d}x^* \tag{95}$$

where $E$ is Young modulus, $A$ is the area of the cross-section, and $I$ denotes the moment of inertia about one of the principal axes of inertia.

On the other hand, the kinetic energy is given by

$$T = \frac{1}{2}\int_0^\ell \rho A\left(\dot{v}^*\right)^2 \mathrm{d}x^* + \frac{1}{2}m\left(\dot{v}^*(x_1^*)\right)^2 \tag{96}$$

where $\rho$ is the beam mass density, $m$ is the lumped mass, and the dot indicates differentiation with respect to the dimensional time $t^*$.

The linear eigenvalue problem yielding the natural frequencies and the associated linear normal modes is solved assuming the solutions in the form

$$v^*(x^*, t^*) \approx \sum_{j=1}^{N^*} \eta_j^*(t^*) \sin j\pi \frac{x^*}{\ell} \tag{97}$$

where $N^*$ is the number of discretizing admissible functions. Substituting (97) and its derivatives into (95) and (96), neglecting nonlinear terms and writing the Euler–Lagrange equations associated with the system Lagrangian, $L = T - V$, yields a set of ordinary-differential equations where the $j$th equation in the generalized coordinates $\eta_k$ is

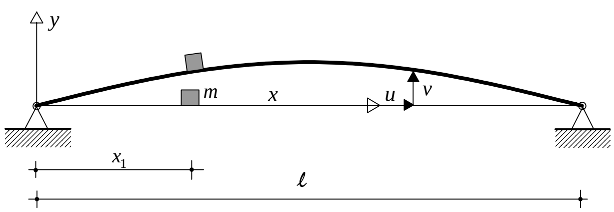


Fig. 1. The hinged–hinged beam geometry with the lumped mass.

$$\rho A \ell \ddot{\eta}_j^* + 2m\left(\sum_{k=1}^{N^*} \ddot{\eta}_k^* \sin k\pi \frac{x_1^*}{\ell}\right) \sin j\pi \frac{x_1^*}{\ell} + \frac{EI}{\ell^3}\pi^4 j^4 \eta_j^* = 0 \tag{98}$$

To render the equations nondimensional, we introduce the following nondimensional variables and parameters: $x = x^*/\ell$, $v = v^*/\ell$, $x_1 = x_1^*/\ell$, $t = \omega_b t^*$, $\omega_b = \sqrt{EI/(\rho A \ell^4)}$, and $\mu = m/(\rho A \ell)$. Then, Eq. (98) can be rewritten in nondimensional form as

$$\ddot{\eta}_j + 2\mu\left(\sum_{k=1}^{N^*} \ddot{\eta}_k \sin k\pi x_1\right) \sin j\pi x_1 + \pi^4 j^4 \eta_j = 0 \tag{99}$$

In turn, the set of equations (99) is rewritten in matrix form as

$$\mathbf{M}\ddot{\boldsymbol{\eta}} + \mathbf{K}\boldsymbol{\eta} = \mathbf{0} \tag{100}$$

where $\mathbf{M}$ and $\mathbf{K}$ are the $N^* \times N^*$ mass and stiffness matrices, respectively. Seeking periodic and synchronous motions, we let $\boldsymbol{\eta} = \exp(\mathrm{i}\omega t)\mathbf{u}$ and obtain the algebraic eigenvalue problem in the standard form

$$\left(\mathbf{K} - \omega^2 \mathbf{M}\right)\mathbf{u} = \mathbf{0} \tag{101}$$

where $(\omega, \mathbf{u})$ is the eigenpair. The beam mode shapes are then expressed as

$$\Phi_j(x) = \sum_{k=1}^{N^*} u_{jk} \sin k\pi x \tag{102}$$

In Fig. 2, variation of the lowest seven calculated nondimensional natural frequencies with the nondimensional mass position $x_1$ is shown when the mass ratio is $\mu = 10$. Because the $k$th linear mode of the beam without the lumped mass possesses $(k-1)$ nodes of vibration at $x_n = 1/k, 2/k, \ldots, (k-1)/k$, when the lumped mass position is $x_1 = x_n$, the corresponding beam frequency is not affected by the lumped mass as confirmed by the numerical results in Fig. 2. Further, inspecting Fig. 2, it is worth noting that, as expected,

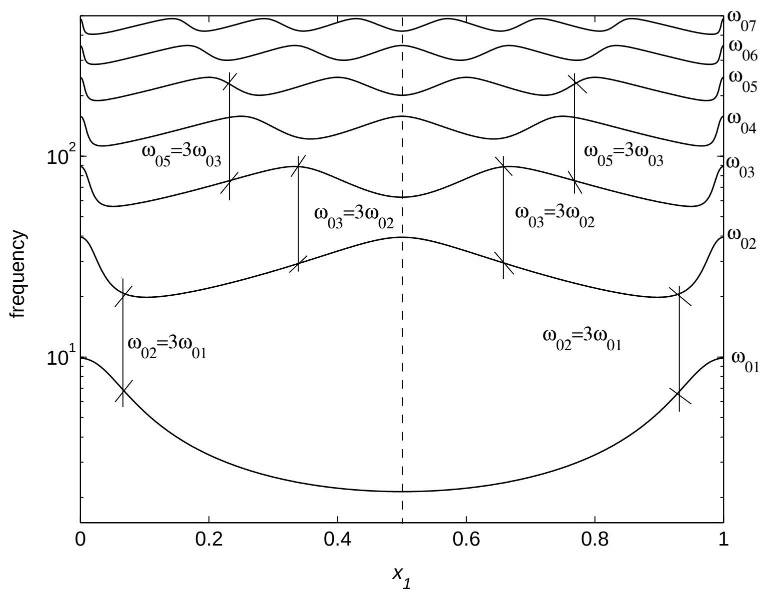


Fig. 2. Variation of the lowest seven nondimensional natural frequencies with $x_1$ when $\mu = 10$. The frequency axis is in log scale.

Table 1
Some cases where three-to-one internal resonances may occur

| $m, n$ | $\omega_{0k}$ | $\mu$ | $x_1$ |
|---|---|---|---|
| 1, 2 | $\omega_{02} = 3\omega_{01} = 21.00$ | 10 | (0.0637, 0.9363) |
| 3, 5 | $\omega_{05} = 3\omega_{03} = 226.70$ | 10 | (0.2335, 0.7665) |
| 2, 3 | $\omega_{03} = 3\omega_{02} = 88.50$ | 10 | (0.3432, 0.6568) |
| 4, 7 | $\omega_{07} = 3\omega_{04} = 473.74$ | 0.024 | 0.5 |

no one-to-one internal resonances occur, while a few three-to-one internal resonances may occur. In Table 1, there are reported the values of the mass ratio $\mu$ and mass position $x_1$ for which three-to-one internal resonances are possible.

As already mentioned in Sections 2 and 3, the nonlinear normal modes are sought as a superposition of the linear normal modes in the form given by (47). Substituting (47) into the system Lagrangian and writing the associated Euler–Lagrange equations, the nonlinear problem is cast in the form of Eq. (2) where the $i$th equation, in nondimensional form, is

$$\ddot{q}_i + \omega_{0i}^2 q_i = -\frac{\lambda^2}{2} \sum_{j=1}^{N} \sum_{k=1}^{N} \sum_{h=1}^{N} q_j q_k q_h \left( \int_0^1 \Phi_j'(x) \Phi_k'(x) \, \mathrm{d}x \right) \left( \int_0^1 \Phi_h'(x) \Phi_i'(x) \, \mathrm{d}x \right) \tag{103}$$

Here, $\lambda$ is the beam slenderness defined as $\lambda = \ell/r$, with $r = \sqrt{I/A}$ denoting the radius of gyration of the cross-section.

The individual mode shapes are expressed by (48) whereas the resonant nonlinear mode shapes are given by (93).

### 5.1. Individual nonlinear normal modes

Three meaningful cases of individual NNM's are considered in the following: (i) $\mu = 0$ (beam without lumped mass); (ii) $\mu = 10$ and $x_1 = 0.5$; (iii) $\mu = 10$ and $x_1 = 0.25$. Solving the linear eigenvalue problem with $N^* = 20$, the nonlinear frequencies of the lowest six modes have been computed according to Eq. (34) and are reported in Tables 2–4. Clearly, the nonlinear frequencies, to within second order, depend on the square of the oscillation amplitude and the beam slenderness. The curves representing variation of the nonlinear frequencies with the amplitude, the so-called backbone curves, are shown for case (i) and $\lambda = 30$ in Fig. 3. In the same figure, representative frequency–response curves are depicted considering weak harmonic forcing and viscous linear damping. The case of weak forcing and light viscous damping can be easily treated letting the forcing and damping terms appear at third order in Eq. (9). It is to be noted that all of the curves, as expected, are bent to the right indicating a hardening behavior (i.e., the oscillation frequency increases with the amplitude). Subsequently, the nonlinear mode shapes have been computed according to Eq. (48) with $N = 10$.

Table 2
Nonlinear frequency laws for the lowest six modes when $\mu = 0$

| $k$ | $\omega_k$ |
|---|---|
| 1 | $\omega_1 = 9.87 + 0.46\lambda^2 a_1^2$ |
| 2 | $\omega_2 = 39.48 + 1.85\lambda^2 a_2^2$ |
| 3 | $\omega_3 = 88.83 + 4.16\lambda^2 a_3^2$ |
| 4 | $\omega_4 = 157.91 + 7.40\lambda^2 a_4^2$ |
| 5 | $\omega_5 = 246.74 + 11.57\lambda^2 a_5^2$ |
| 6 | $\omega_6 = 355.30 + 16.65\lambda^2 a_6^2$ |

Table 3
Nonlinear frequency laws for the lowest six modes when $\mu = 10$ and $x_1 = 0.5$

| $k$ | $\omega_k$ |
|---|---|
| 1 | $\omega_1 = 2.14 + 0.0046\lambda^2 a_1^2$ |
| 2 | $\omega_2 = 39.48 + 1.85\lambda^2 a_2^2$ |
| 3 | $\omega_3 = 62.64 + 1.67\lambda^2 a_3^2$ |
| 4 | $\omega_4 = 157.91 + 7.40\lambda^2 a_4^2$ |
| 5 | $\omega_5 = 202.72 + 7.28\lambda^2 a_5^2$ |
| 6 | $\omega_6 = 355.30 + 16.65\lambda^2 a_6^2$ |

Table 4
Nonlinear frequency laws for the lowest six modes when $\mu = 10$ and $x_1 = 0.25$

| $k$ | $\omega_k$ |
|---|---|
| 1 | $\omega_1 = 2.81 + 0.009\lambda^2 a_1^2$ |
| 2 | $\omega_2 = 24.17 + 0.70\lambda^2 a_2^2$ |
| 3 | $\omega_3 = 78.46 + 3.24\lambda^2 a_3^2$ |
| 4 | $\omega_4 = 157.91 + 7.40\lambda^2 a_4^2$ |
| 5 | $\omega_5 = 213.73 + 7.72\lambda^2 a_5^2$ |
| 6 | $\omega_6 = 309.42 + 12.70\lambda^2 a_6^2$ |

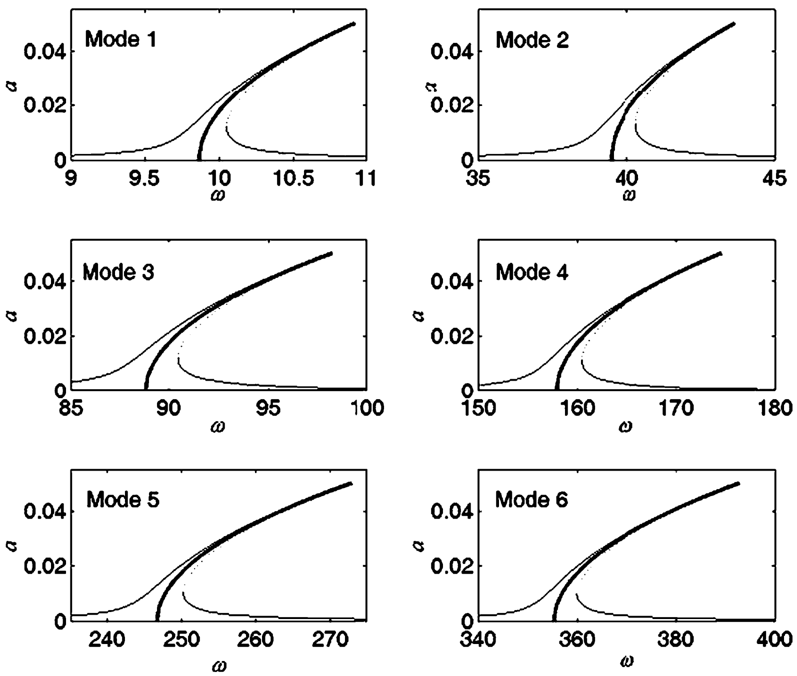


Fig. 3. Backbones of the lowest six modes and representative frequency–response curves when $\mu = 0$.

The case with $\mu = 0$ corresponds to the simply supported uniform beam whose modes are an infinite sequence of symmetric and skew-symmetric modes. Using Eqs. (26) and (28), it turns out that the coefficients $\mathscr{C}_{jk}$ and $\mathscr{D}_{jk}$ are 0 for any $j$ and $k$; this is due to the fact that the work done by the nonlinear restoring

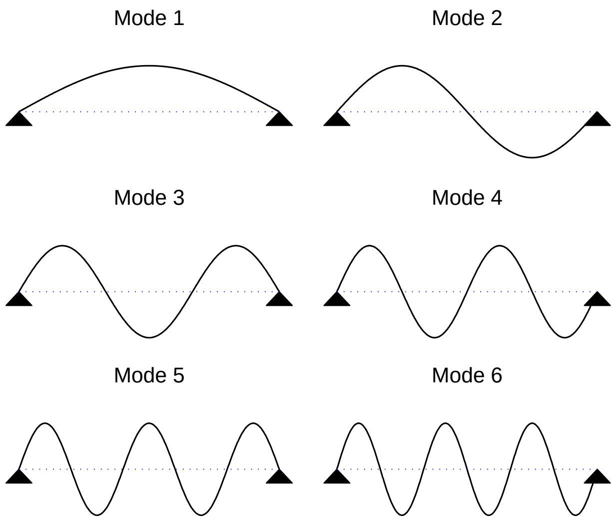


Fig. 4. The lowest six linear normal modes (thin line) and the corresponding individual nonlinear normal modes (thick line) when $\mu = 0$.

force associated with one mode in the virtual displacement associated with any of the other modes vanishes. Consequently, Eq. (48) yields $\mathbf{b}_k = \mathbf{b}_{0k}$ for any $k$ and no difference between the linear and nonlinear modes occurs as confirmed in Fig. 4. The ensuing modes are *similar nonlinear normal modes*. It is worth noting that this result was obtained by Rosenberg (1966) in the general context of homogeneous mechanical systems (i.e., arrays of equal masses and nonlinear springs).

In the same way, both the nonlinear frequencies and corresponding mode shapes have been computed for the second sample beam when $\mu = 10$ and $x_1 = 0.5$. The lowest six calculated backbones are reported in Table 3 and a representation of them, for $\lambda = 30$, is given in Fig. 5 along with some frequency–response curves. On the other hand, in Fig. 6, the lowest six individual nonlinear mode shapes are contrasted with the corresponding linear mode shapes. It is worth pointing out that, since the lumped mass is located at the beam midspan, the mode shapes are either symmetric or skew-symmetric. The mass location is a vibration node for the even modes; therefore, the modal masses of such modes are not influenced by the lumped mass whereas it affects the modal mass of the symmetric modes. This is evident comparing the nonlinear frequency laws with those obtained for the beam without the lumped mass. For the odd modes (i.e., symmetric mode shapes), the effect of the lumped mass is to reduce both the linear modal frequencies and their nonlinear corrections. In fact, in Figs. 5 and 6, we note that the backbone of the first mode is very slightly bent to the right and the difference between the nonlinear mode shape and the linear mode shape is not discernible. On the other hand, the effects of the higher-order symmetric linear mode shapes onto the other symmetric nonlinear mode shapes, such as the third and fifth modes, are evident in their more flexible configurations (Fig. 6).

For the third sample beam ($\mu = 10$ and $x_1 = 0.25$), the computed nonlinear frequency laws are reported in Table 4 and a representation of them is given in Fig. 7. In this case, the modes are neither symmetric nor skew-symmetric. Hence, $(\mathscr{C}_{jk}, \mathscr{D}_{jk}) \neq (0, 0)$; higher-order corrections come into play for both even and odd modes. The comparison between the linear and the nonlinear mode shapes is pictured in Fig. 8. Here, it is to be observed that, for this system, the lumped mass is located in one of the vibration nodes of the fourth mode; therefore, the fourth individual nonlinear normal mode is not influenced by the mass as it can be ascertained comparing its nonlinear frequency law with that obtained for the system without the lumped

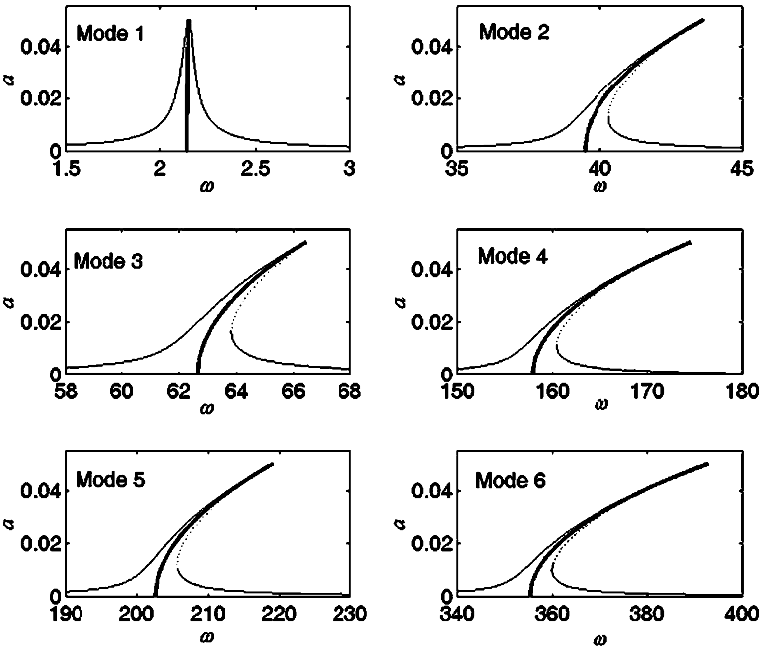


Fig. 5. Backbones of the lowest six modes and representative frequency–response curves when $\mu = 10$ and $x_1 = 0.5$.

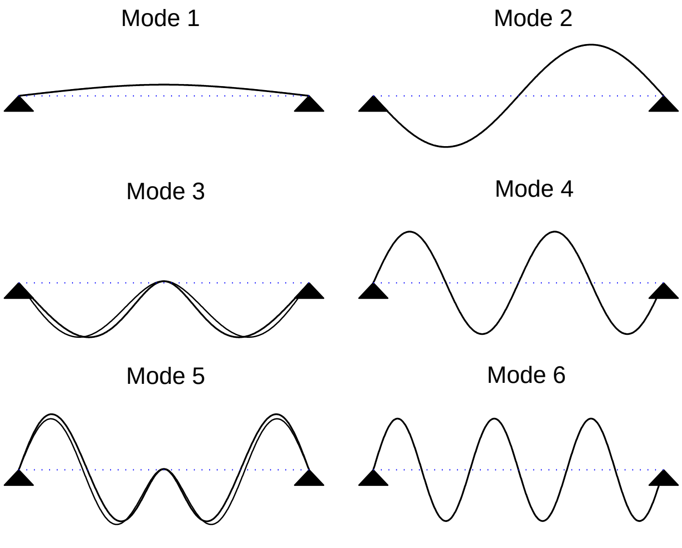


Fig. 6. The lowest six linear normal modes (thin line) and the corresponding individual nonlinear normal modes (thick line) when $\mu = 10$ and $x_1 = 0.5$.

mass and is a similar nonlinear normal mode. For this sample beam, a convergence study has also been conducted to evaluate the effect of the modal truncation on the nonlinear normal modes. In particular, the convergence of the series in Eq. (48) has been tested analyzing the behavior of the coefficients

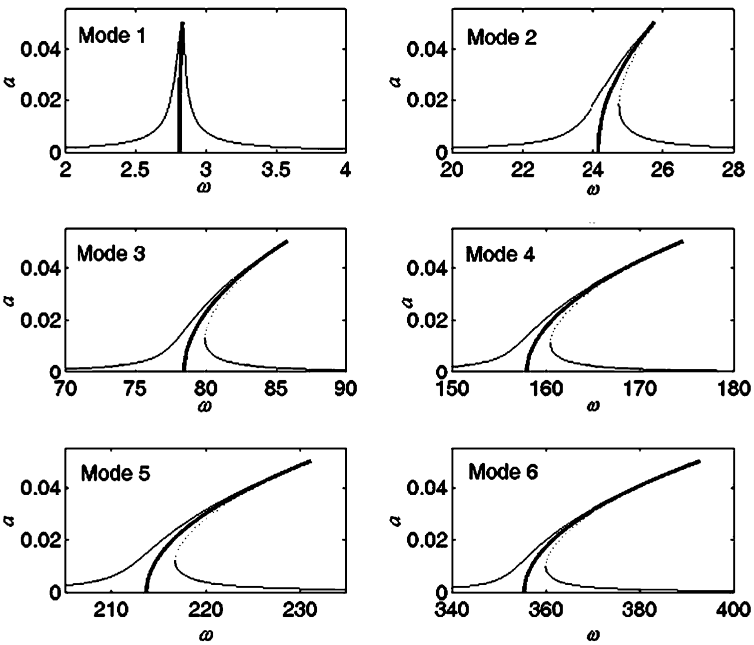


Fig. 7. Lowest six backbones and representative frequency–response curves when $\mu = 10$ and $x_1 = 0.25$.

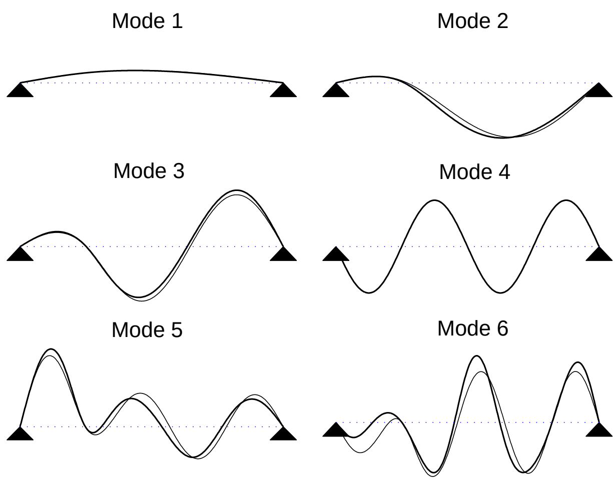


Fig. 8. The lowest six linear normal modes (thin line) and the corresponding individual nonlinear normal modes (thick line) when $\mu = 10$ and $x_1 = 0.25$.

$1/4(\mathscr{C}_{jk} + \mathscr{D}_{jk})$ for increasing mode number up to 15. The results are summarized in Table 5. Practically, convergence is achieved with 10 linear modes for the lowest three NNM's. At the same time, it is interesting to evaluate the relative importance of the nonlinear corrections to the linear characteristics concerning both the frequencies and the mode shapes. To this end, we computed the following quantities:

Table 5
Convergence of the coefficient $1/4(\mathscr{C}_{jk}+\mathscr{D}_{jk})$ in the individual nonlinear mode shapes

| $j$ | Mode $k=1$ | Mode $k=2$ | Mode $k=3$ | Mode $k=5$ | Mode $k=6$ |
|---|---|---|---|---|---|
| 1 | $+0.00\times10^{+00}$ | $+5.20\times10^{-03}$ | $-9.48\times10^{-04}$ | $-4.26\times10^{-04}$ | $2.18\times10^{-04}$ |
| 2 | $-2.67\times10^{-04}$ | $+0.00\times10^{+00}$ | $+5.31\times10^{-03}$ | $+2.70\times10^{-03}$ | $-1.44\times10^{-03}$ |
| 3 | $+1.22\times10^{-05}$ | $-4.09\times10^{-03}$ | $+0.00\times10^{+00}$ | $-4.82\times10^{-03}$ | $+2.58\times10^{-03}$ |
| 4 | $-6.62\times10^{-20}$ | $+1.41\times10^{-16}$ | $+7.38\times10^{-15}$ | $+5.86\times10^{-14}$ | $+4.99\times10^{-15}$ |
| 5 | $+2.22\times10^{-06}$ | $-3.76\times10^{-04}$ | $-4.10\times10^{-04}$ | $+0.00\times10^{+00}$ | $+1.42\times10^{-02}$ |
| 6 | $-7.28\times10^{-07}$ | $+1.26\times10^{-04}$ | $-1.14\times10^{-03}$ | $-8.46\times10^{-03}$ | $+0.00\times10^{+00}$ |
| 7 | $-1.83\times10^{-07}$ | $+3.27\times10^{-05}$ | $-2.50\times10^{-04}$ | $-1.30\times10^{-03}$ | $+3.55\times10^{-03}$ |
| 8 | $+4.29\times10^{-20}$ | $-3.12\times10^{-17}$ | $-2.30\times10^{-16}$ | $-3.98\times10^{-16}$ | $+8.97\times10^{-17}$ |
| 9 | $-1.09\times10^{-07}$ | $+2.01\times10^{-05}$ | $-1.52\times10^{-04}$ | $-2.48\times10^{-03}$ | $+9.78\times10^{-04}$ |
| 10 | $-5.23\times10^{-08}$ | $+9.73\times10^{-06}$ | $-7.42\times10^{-05}$ | $-9.04\times10^{-04}$ | $-7.29\times10^{-03}$ |
| 11 | $-1.91\times10^{-08}$ | $+3.61\times10^{-06}$ | $-2.79\times10^{-05}$ | $-3.13\times10^{-04}$ | $+6.51\times10^{-04}$ |
| 12 | $+2.08\times10^{-21}$ | $-1.10\times10^{-18}$ | $+1.44\times10^{-17}$ | $-2.62\times10^{-17}$ | $-9.98\times10^{-19}$ |
| 13 | $-1.68\times10^{-08}$ | $+3.20\times10^{-06}$ | $-2.51\times10^{-05}$ | $-2.76\times10^{-04}$ | $+4.88\times10^{-04}$ |
| 14 | $+9.34\times10^{-09}$ | $-1.79\times10^{-06}$ | $+1.42\times10^{-05}$ | $+1.56\times10^{-04}$ | $-2.70\times10^{-04}$ |
| 15 | $+4.04\times10^{-09}$ | $-7.80\times10^{-07}$ | $+6.20\times10^{-06}$ | $+6.86\times10^{-05}$ | $-1.18\times10^{-04}$ |

Table 6
Percent variation of the frequencies and the nonlinear mode shapes

| Mode $k$ | $\Delta\omega_k\%$ | $\Delta\Psi_k\%$ |
|---|---|---|
| 1 | 0.32 | 0.56 |
| 2 | 2.89 | 3.77 |
| 3 | 4.13 | 3.23 |
| 4 | 4.69 | 0.00 |
| 5 | 3.61 | 14.31 |
| 6 | 4.10 | 18.08 |

$$\Delta\omega_k\% = \frac{\omega_k-\omega_{0k}}{\omega_{0k}}\frac{1}{(a_k\lambda)^2}\% = -\frac{\alpha_{kkk}}{\omega_{0k}\lambda^2}\% \tag{104}$$

and

$$|\Delta\Psi_k|\% = \max\left|\frac{\Psi_k-\Phi_k}{\Phi_k}\right|\frac{1}{(a_k\lambda)^2}\% = \max\left|\frac{\sum_{j=1,j\neq k}^{N}\left(\mathscr{C}_{jk}+\mathscr{D}_{jk}\right)\Phi_j}{4\Phi_k}\right|\frac{1}{\lambda^2}\% \tag{105}$$

in $x\in[0,1]$. These quantities, reported in Table 6, allow to estimate the relative nonlinear deviation from the linear characteristics; to make the results general, they have been divided by the square of the beam slenderness and oscillation amplitude. For example, for the lowest four modes, $\Delta\omega_k\%=\mathrm{O}(1)$ and $|\Delta\Psi_k|\%=\mathrm{O}(1)$; consequently, the actual frequency and mode shape variations are $\mathrm{O}((a_k\lambda)^2)$. Hence, considering, e.g., $a_k=0.05$ and $\lambda=30$, the percent variation is $\mathrm{O}(1)$.

### 5.2. Resonant nonlinear normal modes

A three-to-one internal resonance between the lowest two modes, occurring in a beam carrying a large mass whose center is in a slight offset with respect to the beam supports ($\mu=10$ and $x_1=0.0637$), has been investigated. Variation of the amplitude ratio $c$ with the normalized detuning $\sigma^*$ has been evaluated according to (71), while the stability of the solutions has been ascertained using (76). For beams with $\lambda=30$, the calculated curve is shown in Fig. 9. Inspecting this figure, it is to be pointed out that, depending

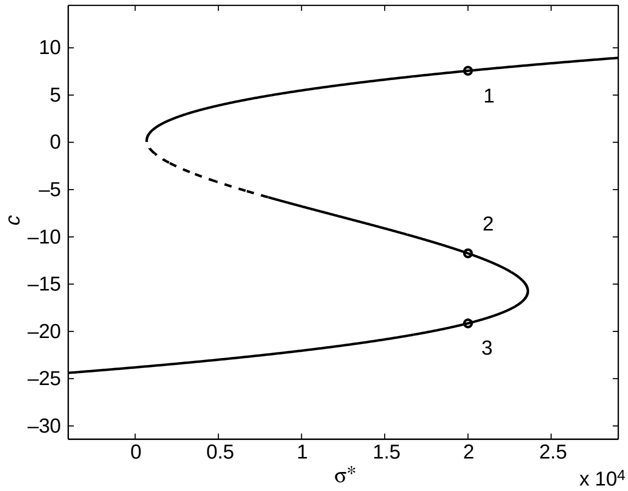


Fig. 9. Variation of the amplitude ratio $c$ with the normalized resonance detuning $\sigma^*$ when $\mu = 10$ and $x_1 = 0.0637$.

on the range of the detuning parameter $\sigma^*$, the beam may possess (i) one stable resonant NNM, (ii) one unstable and two stable resonant NNM's and (iii) three stable resonant NNM's. The computed range of $c$ where unstable and stable NNM's coexist is [−5.7865, 0.091]. The number of nonlinear normal modes is greater than the number of linear normal modes involved in the resonance in agreement with the results of Nayfeh et al. (1996), King and Vakakis (1996), Nayfeh et al. (1999), and Lacarbonara et al. (2003). It is also to be noted that, since the involved frequencies are O(10) (i.e., $\omega_{02} = 21.03$), the detuning parameter $\sigma$ must be $O(1)$ as, in fact, this was assumed in the analysis; therefore, taking into account that $\sigma^* = \sigma/a_n^2 = O(10^4)$ as inferred from Fig. 9, the amplitude $a_n$ must be $O(10^{-2})$. This is consistent with the considered range of variation of the oscillation amplitudes in the backbones of the individual NNM's (Figs. 3, 5, and 7).

According to (80) and (81), the curves $\omega_1 - c$ and $\omega_2 - c$ have been computed and pictured in Fig. 10. Considering, for example, the detuning $\sigma^* = 2 \times 10^4$, then the beam exhibits three stable resonant NNM's marked 1, 2, and 3 in Figs. 9 and 10. It is interesting to appreciate the difference in the nonlinear frequencies associated with the coexisting NNM's, especially between those marked 2 and 3. Furthermore, it is of interest to evaluate the different signatures of the coexisting stable NNM's in the corresponding mode shapes. It is important, however, to preliminarily assess the convergence properties of the nonlinear coefficients $\alpha_{mj}$ and $\alpha_{nj}$ in Eq. (93). Considering the lowest 15 modes, the obtained convergence results are reported in Table 7. The convergence is practically attained with six modes; we further observe that $\alpha_{mj}$ converges faster than $\alpha_{nj}$ does. We also note that, for the NNM denoted with 3, the nonlinear coefficient is $O(10^3)$ whereas the relative amplitude $c$, determining the amplitude of the nonlinear mode at first order, is $O(10)$. However, because the nonlinear correction at second order depends on the square of $a_n$, when the amplitude $a_n$ is $O(10^{-2})$, the nonlinear correction becomes $O(10^{-1})$. This is consistent with the performed perturbation analysis.

Retaining the lowest 10 modes, the calculated resonant nonlinear mode shapes are shown with thick solid lines in Figs. 11(b)–(d) whereas the thin solid lines indicate the interacting first and second linear normal modes in Figs. 11(a)–(d). In the resonant nonlinear mode shapes, the contribution of the higher modes, namely the third, fourth, and fifth linear modes, is clear. This is particularly evident in the NNM in Fig. 11(d).

Similar features have been found in the resonant NNM's arising from other three-to-one internal resonances although the results are not reported for sake of conciseness. Finally, it is pointed out that there are

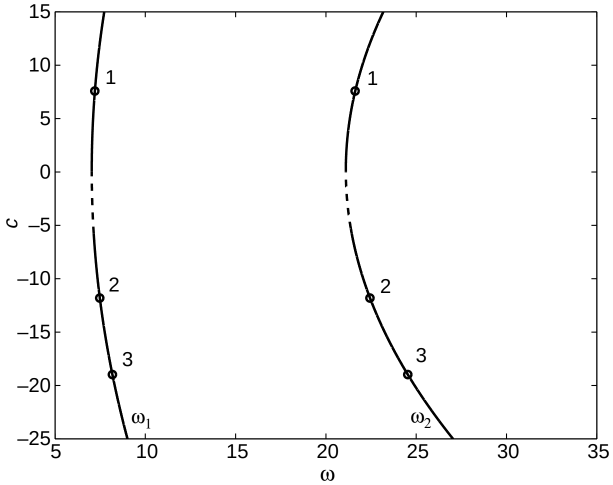


Fig. 10. Variation of the frequencies $\omega_1$ and $\omega_2$ with the amplitude ratio $c$ when $\mu = 10$ and $a = 0.005$.

Table 7
Convergence of the coefficients in the resonant nonlinear mode shapes

| Mode $j$ | $\alpha_{mj}$ | $\alpha_{nj}$ | $(c^3\alpha_{mj} + \alpha_{nj})$ | | |
|---|---|---|---|---|---|
| | | | $c = 7.57$ | $c = -11.74$ | $c = -19.15$ |
| 3 | $+3.90\times10^{-1}$ | $-5.39\times10^{-1}$ | $+1.69\times10^{+2}$ | $-6.47\times10^{+2}$ | $-2.65\times10^{+3}$ |
| 4 | $+6.04\times10^{-2}$ | $+7.22\times10^{-1}$ | $+2.70\times10^{+1}$ | $-9.94\times10^{+1}$ | $-4.09\times10^{+2}$ |
| 5 | $+1.53\times10^{-2}$ | $+1.86\times10^{-1}$ | $+6.84\times10^{+0}$ | $-2.52\times10^{+1}$ | $-1.04\times10^{+2}$ |
| 6 | $-5.16\times10^{-3}$ | $-6.53\times10^{-2}$ | $-2.31\times10^{+0}$ | $+8.49\times10^{+0}$ | $+3.49\times10^{+1}$ |
| 7 | $+2.08\times10^{-3}$ | $+2.72\times10^{-2}$ | $+9.33\times10^{-1}$ | $-3.43\times10^{+0}$ | $-1.41\times10^{+1}$ |
| 8 | $-9.55\times10^{-4}$ | $-1.28\times10^{-2}$ | $-4.28\times10^{-1}$ | $+1.57\times10^{+0}$ | $+6.47\times10^{+0}$ |
| 9 | $+4.79\times10^{-4}$ | $+6.51\times10^{-3}$ | $+2.15\times10^{-1}$ | $-7.88\times10^{-1}$ | $-3.24\times10^{+0}$ |
| 10 | $-2.56\times10^{-4}$ | $-3.53\times10^{-3}$ | $-1.15\times10^{-1}$ | $+4.21\times10^{-1}$ | $+1.73\times10^{+0}$ |
| 11 | $+1.43\times10^{-4}$ | $+1.99\times10^{-3}$ | $+6.41\times10^{-2}$ | $-2.35\times10^{-1}$ | $-9.68\times10^{-1}$ |
| 12 | $-8.17\times10^{-5}$ | $-1.15\times10^{-3}$ | $-3.66\times10^{-2}$ | $+1.34\times10^{-1}$ | $+5.53\times10^{-1}$ |
| 13 | $-4.63\times10^{-5}$ | $-6.54\times10^{-4}$ | $-2.08\times10^{-2}$ | $+7.61\times10^{-2}$ | $+3.13\times10^{-1}$ |
| 14 | $+2.43\times10^{-5}$ | $+3.46\times10^{-4}$ | $+1.09\times10^{-2}$ | $-4.00\times10^{-2}$ | $-1.65\times10^{-1}$ |
| 15 | $-9.08\times10^{-6}$ | $-1.30\times10^{-4}$ | $-4.08\times10^{-3}$ | $+1.49\times10^{-2}$ | $+6.15\times10^{-2}$ |

cases where, although the linear frequencies are commensurable with a 3:1 integer ratio, the interaction does not actually occur. It is, for instance, the last case in Table 1, where $\omega_{07} = 3\omega_{04} = 473.74$; in fact, the orthogonality condition $\mathbf{u}_7^{\mathrm{T}}\mathbf{b}_{444} = 0$ is satisfied and the two modes happen to be nonresonant.

## 6. Conclusions

In this paper, an analytical construction of the nonlinear normal modes of general multi-degree-of-freedom self-adjoint structural systems with weak cubic geometric and inertia nonlinearities has been pursued. The employed asymptotic approach, based on the method of multiple scales, attempts to generalize previous studies in that it systematically leads to the closed-form invariant manifolds and the nonlinear mode shapes (nonlinear eigenvectors) as an extension of the linear counterparts. These modes

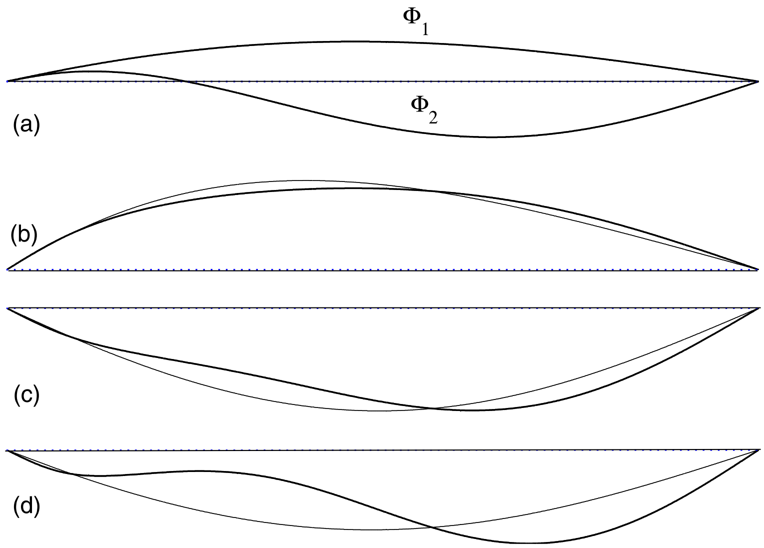


Fig. 11. (a) The lowest two linear mode shapes when $x_1 = 0.0637$ and $\mu = 10$ and (b)–(d) the resonant nonlinear mode shapes (thick lines) superimposed on their first-order parts (thin lines) corresponding to the solutions marked 1 (b), 2 (c), and 3 (d) in Figs. 9 and 10.

have been calculated away from internal resonances—individual nonlinear normal modes—and in their vicinity—resonant nonlinear normal modes. The employed operator notation makes the results general and the computational implementation effective also with large systems.

The motivation for employing the asymptotic approach lies in the fact that the closed-form NNM's can be used to investigate general properties of certain classes of structural systems undergoing moderately large vibration amplitudes. Along these lines, closed-form conditions were determined for systems possessing similar normal modes. Further, the obtained closed-form NNM's are amenable to be exploited for nonlinear modal-type analyses of general self-adjoint structural systems with many degrees of freedom.

To corroborate the presented theoretical results, an illustrative example has been discussed, a hinged–hinged uniform elastic beam carrying a lumped mass. Depending on the lumped mass relative to the beam mass and on its location along the beam, different classes of individual and resonant NNM's have been found. The differences can be remarkable as in the case when the mass is at the midspan with respect to the case when it is in some other locations. While with the mass at the midspan, the NNM's preserve the symmetric and skew-symmetric nature of the linear normal modes and the symmetric NNM's only are affected by higher-order modal contributions, in other mass locations along the span, the modes are hybrid and are always affected by the nonlinear stretching effect activating a funicular load-carrying mechanism. In addition, the general convergence properties of the nonlinear mode shapes have been discussed. The results also indicate that different reduced-order models must be knowledgeably constructed using the obtained NNM's depending on the inertial-geometric features of the considered beam as in more general structures.

## Acknowledgements

This work was partially supported by the FY-2002 Giovani Ricercatori Grant (Young Investigators Grant) from the University of Rome La Sapienza.

## Appendix A

### A.1. Higher-order functions

Substituting (62) and (63) into (51) and (52), and equating the coefficients of like harmonic terms to 0, the following set of 16 algebraic problems is obtained:

$$\omega_{0m}\mathbf{z}_1 - \tilde{\mathbf{w}}_1 = \frac{1}{2\omega_{0m}}\mathbf{u}_m^{\mathrm{T}}\mathbf{R}_{mn}\mathbf{u}_m \tag{A.1}$$

$$-\omega_{0m}\tilde{\mathbf{w}}_1 + \boldsymbol{\Lambda}\mathbf{z}_1 = -\tfrac{1}{2}\mathbf{u}_m^{\mathrm{T}}\mathbf{R}_{mn}\mathbf{u}_m + \mathbf{R}_{mn} \tag{A.2}$$

$$\omega_{0m}\mathbf{z}_3 - \tilde{\mathbf{w}}_3 = \frac{1}{2\omega_{0m}}\boldsymbol{\Gamma}_{mmm}\mathbf{u}_m \tag{A.3}$$

$$-\omega_{0m}\tilde{\mathbf{w}}_3 + \boldsymbol{\Lambda}\mathbf{z}_3 = -\tfrac{1}{2}\boldsymbol{\Gamma}_{mmm}\mathbf{u}_m + \mathbf{a}_{mmm} \tag{A.4}$$

$$(\omega_{0n} - 2\omega_{0m})\mathbf{z}_5 - \tilde{\mathbf{w}}_5 = \frac{1}{2\omega_{0m}}\mathbf{u}_m^{\mathrm{T}}\mathbf{S}_{mn}\mathbf{u}_m \tag{A.5}$$

$$-(\omega_{0n} - 2\omega_{0m})\tilde{\mathbf{w}}_5\boldsymbol{\Lambda}\mathbf{z}_5 = -\tfrac{1}{2}\mathbf{u}_m^{\mathrm{T}}\mathbf{S}_{mn}\mathbf{u}_m + \mathbf{S}_{mn} \tag{A.6}$$

$$\omega_{0n}\mathbf{z}_2 - \tilde{\mathbf{w}}_2 = \frac{1}{2\omega_{0n}}\mathbf{u}_n^{\mathrm{T}}\mathbf{R}_{nm}\mathbf{u}_n \tag{A.7}$$

$$-\omega_{0n}\tilde{\mathbf{w}}_2 + \boldsymbol{\Lambda}\mathbf{z}_2 = -\tfrac{1}{2}\mathbf{u}_n^{\mathrm{T}}\mathbf{R}_{nm}\mathbf{u}_n + \mathbf{R}_{nm} \tag{A.8}$$

$$\omega_{0n}\mathbf{z}_4 - \tilde{\mathbf{w}}_4 = \frac{1}{2\omega_{0n}}\boldsymbol{\Gamma}_{nnn}\mathbf{u}_n \tag{A.9}$$

$$-\omega_{0n}\tilde{\mathbf{w}}_4 + \boldsymbol{\Lambda}\mathbf{z}_4 = -\tfrac{1}{2}\boldsymbol{\Gamma}_{nnn}\mathbf{u}_n + \mathbf{a}_{nnn} \tag{A.10}$$

$$3\omega_{0m}\mathbf{z}_7 - \tilde{\mathbf{w}}_7 = \frac{1}{2\omega_{0n}}\mathbf{u}_n^{\mathrm{T}}\mathbf{b}_{mmm}\mathbf{u}_n \tag{A.11}$$

$$-3\omega_{0m}\tilde{\mathbf{w}}_7 + \boldsymbol{\Lambda}\mathbf{z}_7 = -\tfrac{1}{2}\mathbf{u}_n^{\mathrm{T}}\mathbf{b}_{mmm}\mathbf{u}_n + \mathbf{b}_{mmm} \tag{A.12}$$

$$(2\omega_{0n} - \omega_{0m})\mathbf{z}_6 - \tilde{\mathbf{w}}_6 = \mathbf{0} \tag{A.13}$$

$$-(2\omega_{0n} - \omega_{0m})\tilde{\mathbf{w}}_6 + \boldsymbol{\Lambda}\mathbf{z}_6 = \mathbf{S}_{nm} \tag{A.14}$$

$$3\omega_{0n}\mathbf{z}_8 - \tilde{\mathbf{w}}_8 = \mathbf{0} \tag{A.15}$$

$$-3\omega_{0n}\tilde{\mathbf{w}}_8 + \boldsymbol{\Lambda}\mathbf{z}_8 = \mathbf{b}_{nnn} \tag{A.16}$$

The solutions of (A.1)–(A.16) are

$$\mathbf{z}_1 = \frac{1}{4\omega_{0m}^2}(\mathbf{u}_m^{\mathrm{T}}\mathbf{R}_{mn})\mathbf{u}_m + \sum_{j=1, j\neq m}^{N}\frac{\mathbf{u}_j^{\mathrm{T}}\mathbf{R}_{mn}}{\omega_{0j}^2 - \omega_{0m}^2}\mathbf{u}_j \tag{A.17}$$

$$\tilde{\mathbf{w}}_1 = -\frac{1}{4\omega_{0m}}(\mathbf{u}_m^{\mathrm{T}}\mathbf{R}_{mn})\mathbf{u}_m + \omega_{0m}\sum_{j=1, j\neq m}^{N}\frac{\mathbf{u}_j^{\mathrm{T}}\mathbf{R}_{mn}}{\omega_{0j}^2 - \omega_{0m}^2}\mathbf{u}_j \tag{A.18}$$

$$\mathbf{z}_2 = \frac{1}{4\omega_{0n}^2}(\mathbf{u}_n^{\mathrm{T}}\mathbf{R}_{nm})\mathbf{u}_n + \sum_{j=1, j\neq n}^{N}\frac{\mathbf{u}_j^{\mathrm{T}}\mathbf{R}_{nm}}{\omega_{0j}^2 - \omega_{0n}^2}\mathbf{u}_j \tag{A.19}$$

$$\tilde{\mathbf{w}}_2 = -\frac{1}{4\omega_{0n}}(\mathbf{u}_n^{\mathrm{T}}\mathbf{R}_{nm})\mathbf{u}_n + \omega_{0n}\sum_{j=1, j\neq n}^{N}\frac{\mathbf{u}_j^{\mathrm{T}}\mathbf{R}_{nm}}{\omega_{0j}^2 - \omega_{0n}^2}\mathbf{u}_j \tag{A.20}$$

$$\mathbf{z}_3 = \frac{1}{4\omega_{0m}^2}\Gamma_{mmm}\mathbf{u}_m + \sum_{j=1, j\neq m}^{N}\frac{\mathbf{u}_j^{\mathrm{T}}\mathbf{a}_{mmm}}{\omega_{0j}^2 - \omega_{0m}^2}\mathbf{u}_j \tag{A.21}$$

$$\tilde{\mathbf{w}}_3 = -\frac{1}{4\omega_{0m}}\Gamma_{mmm}\mathbf{u}_m + \omega_{0m}\sum_{j=1, j\neq m}^{N}\frac{\mathbf{u}_j^{\mathrm{T}}\mathbf{a}_{mmm}}{\omega_{0j}^2 - \omega_{0m}^2}\mathbf{u}_j \tag{A.22}$$

$$\mathbf{z}_4 = \frac{1}{4\omega_{0n}^2}\Gamma_{nnn}\mathbf{u}_n + \sum_{j=1, j\neq n}^{N}\frac{\mathbf{u}_j^{\mathrm{T}}\mathbf{a}_{nnn}}{\omega_{0j}^2 - \omega_{0n}^2}\mathbf{u}_j \tag{A.23}$$

$$\tilde{\mathbf{w}}_4 = -\frac{1}{4\omega_{0n}}\Gamma_{nnn}\mathbf{u}_n + \omega_{0n}\sum_{j=1, j\neq n}^{N}\frac{\mathbf{u}_j^{\mathrm{T}}\mathbf{a}_{nnn}}{\omega_{0j}^2 - \omega_{0n}^2}\mathbf{u}_j \tag{A.24}$$

$$\mathbf{z}_5 = \frac{1}{4\omega_{0m}^2}(\mathbf{u}_m^{\mathrm{T}}\mathbf{S}_{mn})\mathbf{u}_m + \sum_{j=1, j\neq m}^{N}\frac{\mathbf{u}_j^{T}\mathbf{S}_{mn}}{\omega_{0j}^2 - \omega_{0m}^2}\mathbf{u}_j \tag{A.25}$$

$$\tilde{\mathbf{w}}_5 = -\frac{1}{4\omega_{0m}}(\mathbf{u}_m^{\mathrm{T}}\mathbf{S}_{mn})\mathbf{u}_m + \omega_{0m}\sum_{j=1, j\neq m}^{N}\frac{\mathbf{u}_j^{\mathrm{T}}\mathbf{S}_{mn}}{\omega_{0j}^2 - \omega_{0m}^2}\mathbf{u}_j \tag{A.26}$$

$$\mathbf{z}_6 = \sum_{j=1}^{N}\frac{\mathbf{u}_j^{\mathrm{T}}\mathbf{S}_{nm}}{\omega_{0j}^2 - 25\omega_{0m}^2}\mathbf{u}_j \tag{A.27}$$

$$\tilde{\mathbf{w}}_6 = (2\omega_{0n} - \omega_{0m})\sum_{j=1}^{N}\frac{\mathbf{u}_j^{\mathrm{T}}\mathbf{S}_{nm}}{\omega_{0j}^2 - 25\omega_{0m}^2}\mathbf{u}_j \tag{A.28}$$

$$\mathbf{z}_7 = \frac{1}{4\omega_{0m}^2}(\mathbf{u}_n^{\mathrm{T}}\mathbf{b}_{mmm})\mathbf{u}_n + \sum_{j=1, j\neq n}^{N}\frac{\mathbf{u}_j^{\mathrm{T}}\mathbf{b}_{mmm}}{\omega_{0j}^2 - \omega_{0n}^2}\mathbf{u}_j \tag{A.29}$$

$$\tilde{\mathbf{w}}_7 = -\frac{1}{4\omega_{0m}}(\mathbf{u}_n^{\mathrm{T}}\mathbf{b}_{mmm})\mathbf{u}_n + \omega_{0m}\sum_{j=1, j\neq n}^{N}\frac{\mathbf{u}_j^{\mathrm{T}}\mathbf{b}_{mmm}}{\omega_{0j}^2 - \omega_{0n}^2}\mathbf{u}_j \tag{A.30}$$

$$\mathbf{z}_8 = \sum_{j=1}^{N} \frac{\mathbf{u}_j^{\mathrm{T}} \mathbf{b}_{nnn}}{\omega_{0j}^2 - 9\omega_{0n}^2} \mathbf{u}_j \tag{A.31}$$

$$\tilde{\mathbf{w}}_8 = 3\omega_{0n} \sum_{j=1}^{N} \frac{\mathbf{u}_j^{\mathrm{T}} \mathbf{b}_{nnn}}{\omega_{0j}^2 - 9\omega_{0n}^2} \mathbf{u}_j \tag{A.32}$$

### A.2. Coefficients appearing in the invariant manifolds

Substituting Eqs. (A.17)–(A.32) into (82) and (83), the coefficients of (86) and (87) can be expressed as

$$r_{1j} = \frac{\mathbf{u}_j^{\mathrm{T}} \mathbf{R}_{mn}}{4(\omega_{0j}^2 - \omega_{0m}^2)} \tag{A.33}$$

$$r_{2j} = \frac{\mathbf{u}_j^{\mathrm{T}} \mathbf{R}_{nm}}{4(\omega_{0j}^2 - \omega_{0n}^2)} \tag{A.34}$$

$$r_{3j} = \frac{\mathbf{u}_j^{\mathrm{T}} \mathbf{a}_{mmm}}{4(\omega_{0j}^2 - \omega_{0m}^2)} \tag{A.35}$$

$$r_{4j} = \frac{\mathbf{u}_j^{\mathrm{T}} \mathbf{a}_{nnn}}{4(\omega_{0j}^2 - \omega_{0n}^2)} \tag{A.36}$$

$$r_{5j} = \frac{\mathbf{u}_j^{\mathrm{T}} \mathbf{S}_{mn}}{4(\omega_{0j}^2 - \omega_{0m}^2)} \tag{A.37}$$

$$r_{6j} = \frac{\mathbf{u}_j^{\mathrm{T}} \mathbf{S}_{nm}}{4(\omega_{0j}^2 - 25\omega_{0m}^2)} \tag{A.38}$$

$$r_{7j} = \frac{\mathbf{u}_j^{\mathrm{T}} \mathbf{b}_{mmm}}{4(\omega_{0j}^2 - \omega_{0n}^2)} \tag{A.39}$$

$$r_{8j} = \frac{\mathbf{u}_j^{\mathrm{T}} \mathbf{b}_{nnn}}{4(\omega_{0j}^2 - 9\omega_{0n}^2)} \tag{A.40}$$

$$s_{1j} = -\omega_{0m} \frac{\mathbf{u}_j^{\mathrm{T}} \mathbf{R}_{mn}}{4(\omega_{0j}^2 - \omega_{0m}^2)} \tag{A.41}$$

$$s_{2j} = -\omega_{0n} \frac{\mathbf{u}_j^{\mathrm{T}} \mathbf{R}_{nm}}{4(\omega_{0j}^2 - \omega_{0n}^2)} \tag{A.42}$$

$$s_{3j} = -\omega_{0m} \frac{\mathbf{u}_j^{\mathrm{T}} \mathbf{a}_{mmm}}{4(\omega_{0j}^2 - \omega_{0m}^2)} \tag{A.43}$$

$$s_{4j} = -\omega_{0n} \frac{\mathbf{u}_j^{\mathrm{T}} \mathbf{a}_{nnn}}{4(\omega_{0j}^2 - \omega_{0n}^2)} \tag{A.44}$$

$$s_{5j} = -\omega_{0m} \frac{\mathbf{u}_j^{\mathrm{T}} \mathbf{S}_{mn}}{4(\omega_{0j}^2 - \omega_{0m}^2)} \tag{A.45}$$

$$s_{6j} = -5\omega_{0m} \frac{\mathbf{u}_j^{\mathrm{T}} \mathbf{S}_{nm}}{4(\omega_{0j}^2 - 25\omega_{0m}^2)} \tag{A.46}$$

$$s_{7j} = -\omega_{0m} \frac{\mathbf{u}_j^{\mathrm{T}} \mathbf{b}_{mmm}}{4(\omega_{0j}^2 - \omega_{0n}^2)} \tag{A.47}$$

$$s_{8j} = -3\omega_{0n} \frac{\mathbf{u}_j^{\mathrm{T}} \mathbf{b}_{nnn}}{4(\omega_{0j}^2 - 9\omega_{0n}^2)} \tag{A.48}$$

The coefficients in Eqs. (88) and (89) are

$$\alpha_{1j} = \frac{r_{3j} - 3r_{7j}}{\omega_{0m}^2} \tag{A.49}$$

$$\alpha_{2j} = \frac{2(r_{2j} + 2r_{5j})}{\omega_{0m}\omega_{0n}} \tag{A.50}$$

$$\alpha_{3j} = \frac{2r_{1j}}{\omega_{0n}^2} \tag{A.51}$$

$$\alpha_{mj} = r_{3j} + r_{7j} \tag{A.52}$$

$$\alpha_{5j} = \frac{2r_{2j}}{\omega_{0m}^2} \tag{A.53}$$

$$\alpha_{6j} = \frac{2(r_{1j} + 2r_{6j})}{\omega_{0m}\omega_{0n}} \tag{A.54}$$

$$\alpha_{7j} = \frac{r_{4j} - 3r_{8j}}{\omega_{0n}^2} \tag{A.55}$$

$$\alpha_{nj} = r_{4j} + r_{8j} \tag{A.56}$$

$$\beta_{mj} = \frac{s_{7j} - s_{3j}}{\omega_{0m}^3} \tag{A.57}$$

$$\beta_{2j} = -\frac{2s_{2j}}{\omega_{0m}^2\omega_{0n}} \tag{A.58}$$

$$\beta_{3j} = -\frac{2s_{1j}}{\omega_{0m}\omega_{0n}^2} \tag{A.59}$$

$$\beta_{nj} = \frac{s_{8j} - s_{4j}}{\omega_{0n}^3} \tag{A.60}$$

$$\beta_{5j} = -\frac{s_{3j} + 3s_{7j}}{\omega_{0m}} \tag{A.61}$$

$$\beta_{6j} = \frac{2(s_{2j} + 2s_{5j})}{\omega_{0m}} \tag{A.62}$$

$$\beta_{7j} = \frac{2(s_{1j} - 2s_{6j})}{\omega_{0n}} \tag{A.63}$$

$$\beta_{8j} = -\frac{s_{4j} + 3s_{8j}}{\omega_{0n}} \tag{A.64}$$

## References


Camillacci, R., 2003. Nonlinear Modal Analysis for Systems with Geometric Nonlinearities: Analytical and Experimental Methods. Ph.D. Dissertation, University of Rome Tre, Rome, Italy.

King, M.E., Vakakis, A.F., 1993. An energy-based formulation for computing nonlinear normal modes in undamped continuous systems. Journal of Vibration and Acoustics 116, 332–340.

King, M.E., Vakakis, A.F., 1996. An energy-based approach to computing resonant nonlinear normal modes. Journal of Applied Mechanics 63, 810–819.

Lacarbonara, W., Rega, G., 2003. Resonant nonlinear normal modes. Part II: Activation/orthogonality conditions for shallow structural systems. International Journal of Non-Linear Mechanics 38, 873–887.

Lacarbonara, W., Rega, G., Nayfeh, A.H., 2003. Resonant nonlinear normal modes. Part I: Analytical treatment for structural one-dimensional systems. International Journal of Non-Linear Mechanics 38, 851–872.

Mettler, E., 1962. Dynamic buckling. In: Handbook of Engineering Mechanics. McGraw-Hill, New York.

Nayfeh, A.H., 1995. On direct methods for constructing nonlinear normal modes of continuous systems. Journal of Vibration and Control 1, 389–430.

Nayfeh, A.H., Nayfeh, S.A., 1994. On nonlinear modes of continuous systems. Journal of Vibration and Acoustics 116, 129–136.

Nayfeh, A.H., Nayfeh, S.A., 1995. Nonlinear normal modes of a continuous system with quadratic nonlinearities. Journal of Vibration and Acoustics 117, 199–205.

Nayfeh, A.H., Chin, C.-M., Nayfeh, S.A., 1996. On nonlinear normal modes of systems with internal resonance. Journal of Vibration and Acoustics 111, 340–345.

Nayfeh, A.H., Lacarbonara, W., Chin, C.-M., 1999. Nonlinear normal modes of buckled beams: three-to-one and one-to-one internal resonances. Nonlinear Dynamics 18, 253–273.

Pak, C., Rand, R.H., Moon, F.C., 1992. Free vibrations of a thin elastica by normal modes. Nonlinear Dynamics 3, 347–364.

Pesheck, E., Boivin, N., Pierre, C., Shaw, S.W., 2001. Nonlinear modal analysis of structural systems using multi-mode invariant manifolds. Nonlinear Dynamics 25, 183–205.

Rosenberg, R.M., 1962. The normal modes of nonlinear *n*-degree-of-freedom systems. Journal of Applied Mechanics 30, 7–14.

Rosenberg, R.M., 1966. On nonlinear vibrations of systems with many degrees of freedom. Advances in Applied Mechanics 9, 155–242.

Rand, R.H., 1974. A direct method for non-linear normal modes. International Journal of Non-Linear Mechanics 9, 363–368.

Rand, R.H., Pak, C.H., Vakakis, A.F., 1992. Bifurcation of nonlinear normal modes in a class of two degree of freedom systems. Acta Mechanica 3, 129–146.

Shaw, S.W., Pierre, C., 1991. Non-linear normal modes and invariant manifolds. Journal of Sound and Vibration 150, 170–173.

Shaw, S.W., Pierre, C., 1993. Normal modes for non-linear vibratory systems. Journal of Sound and Vibration 164, 85–124.

Shaw, S.W., Pierre, C., 1994. Normal modes of vibration for non-linear continuous systems. Journal of Sound and Vibration 169, 319–347.

Vakakis, A.F., Rand, R.H., 1992. Normal modes and global dynamics of a two-degree-of-freedom non-linear system-I. Low energies. International Journal of Non-Linear Mechanics 27, 861–874.

Vakakis, A.F., Mikhlin, L.I., Pilipchuk, Yu.V., Zevin, A.A., 1996. Normal Modes and Localization in Nonlinear Systems. Wiley, New York.